ChemPlusChem

Review
doi.org/10.1002/cplu.202400162

Chemistry Europe
European Chemical Societies Publishing

www.chempluschem.org

Recent Advances on the Chemistry of Transition Metal Complexes with Monoanionic Bidentate Silyl Ligands

María Batuecas,*[a] Alejandra Goméz-España,[a, b] and Francisco J. Fernández-Álvarez*[a]

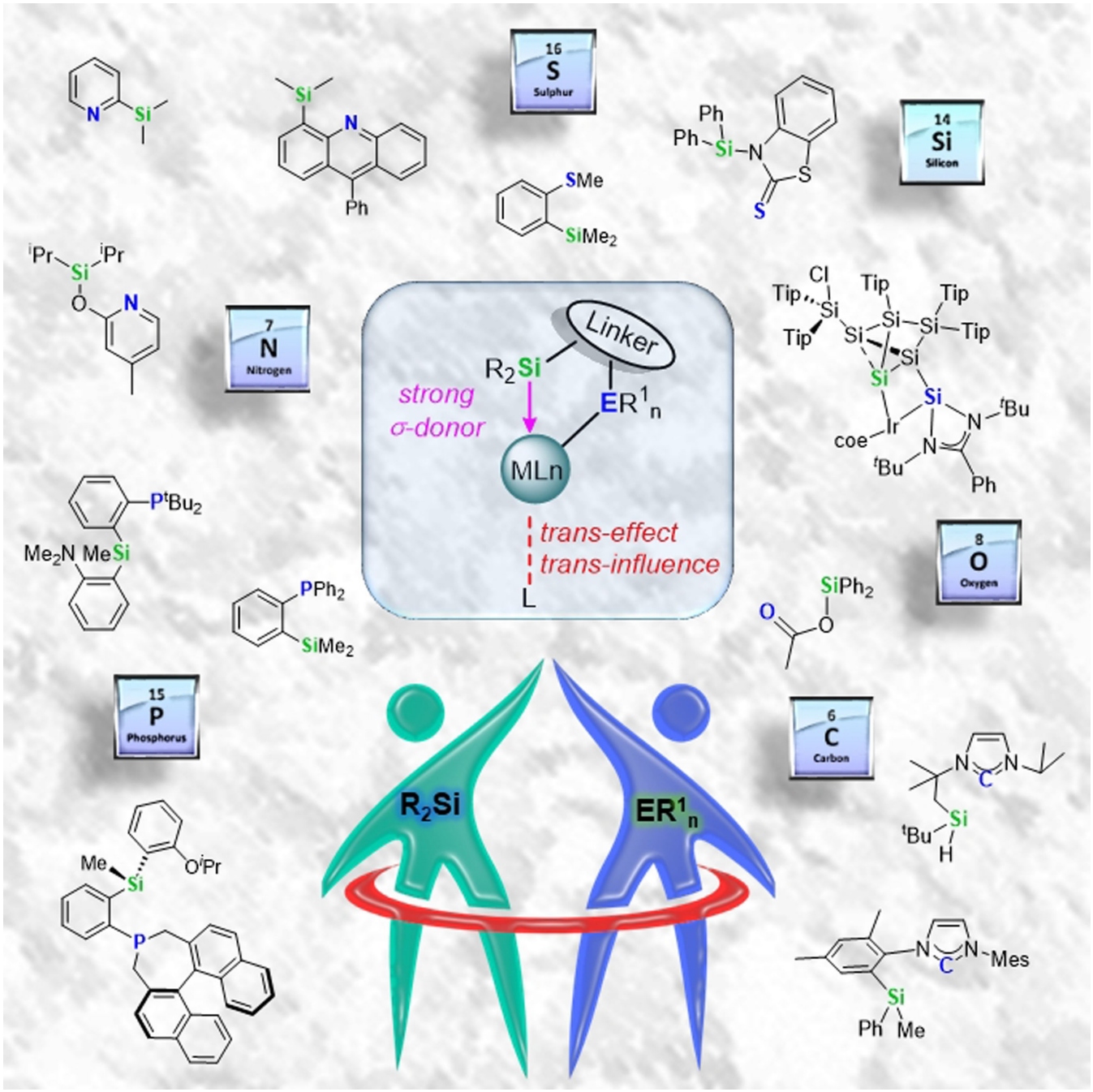

The chemistry of transition-metal (TM) complexes with monoanionic bidentate (κ^2-*L*,*Si*) silyl ligands has considerably grown in recent years. This work summarizes the advances in the chemistry of TM-(κ^2-*L*,*Si*) complexes (*L* = *N*-heterocycle, phosphine, *N*-heterocyclic carbene, thioether, ester, silylether or tetrylene). The most common synthetic method has been the oxidative addition of the Si–H bond to the metal center assisted by the coordination of L. The metal silicon bond distances in TM-(κ^2-*L*,*Si*) complexes are in the range of metal-silyl bond distances. TM-(κ^2-*L*,*Si*) complexes have proven to be effective catalysts for hydrosilylation and/or hydrogenation of unsaturated molecules among other processes.

1. Introduction

One of the foundations of homogeneous catalysis based on transition metal (TM) complexes is that by adjusting the electronic and/or steric properties of the ligands "ligand tuning" it is possible to optimize both the activity and the selectivity of the catalytic processes. That is why the design and development of ligands can be considered one of the most important research topics within homogeneous catalysis.[1]

In this context, the chemistry of TM-complexes with multidentate organosilyl ancillary ligands have considerably grown in the last decades.[2–8] These type of ligands are characterized by their strong σ-donor character, and the high *trans*-effect and -influence of the silyl group which facilitate the generation of electronically and coordinatively unsaturated species.[2–8]

TM-complexes with tetradentate κ^4-*L*$_3$,*Si*,[7] tridentate κ^3-*L*$_2$,*Si*,[4,5,8] and/or bidentate κ^2-*L*,*Si*[6] ligands, where Si symbolizes a silyl group and L represents a σ-donor ligand (*N*-heterocycle, phosphine, *N*-heterocyclic carbene, thioether, ester, silylether or tetrylene), have been reported. Most of the studies on TM-complexes with multidentate silyl ancillary ligands published to date are focused on the chemistry of species with tridentate ligands of type κ^3-*L*,*Si*,*L*, which have been the subject of numerous reviews in recent years.[4,5,8] The chemistry of TM-complexes with monoanionic bidentate κ^2-*L*,*Si* ligands has gained interest in recent years due to their potential as hydrosilylation and hydrogenation homogeneous catalysts. Moreover, some TM-(κ^2-*L*,*Si*) complexes have shown better catalytic performance than their TM-(κ^3-*L*,*Si*,*L*) counterparts in CO_2 hydrosilylation and Kumada coupling reactions. This review describes the recent outcomes of the chemistry of TM-complexes with different κ^2-*L*,*Si* ligands including their synthesis and applications in homogeneous catalysis, as well as some relevant aspects about the nature of the metal–Si bond (Figure 1).

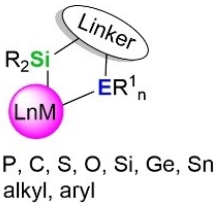

Figure 1. General representation of TM-complexes with κ^2-*L*,*Si* ligands.

This review has been organized into sections in which the ligands have been classified based on the nature of the σ-donor atom (E in Figure 1). In each section, the methodology of synthesis of the ligands and the corresponding complexes are described, as well as some relevant aspects about the structure, reactivity, and catalytic activity. In addition, a final brief discussion about the metal-silicon bond distances in TM-(κ^2-*L*,*Si*) species has also been included.

2. Transition Metal Complexes with κ^2-*L*,*Si* Ligands

2.1. Transition Metal Complexes with κ^2-*N*,*Si* Ligands

To the best of our knowledge the first example of a TM-(κ^2-*N*,*Si*) complex was reported in 1989 by Ang and Kwik. They prepared the complex [Re(κ^2-*N*,*Si*-**L1**)(CO)$_4$] (**L1** = 2-pyridyldimethylsilyl, **1**) by reaction of 2-pyridyldimethylsilane with [Re(CO)$_5$]$_2$ at 433 K. Complex **1** was characterized by means of elemental analysis and infrared spectroscopy (Scheme 1).[9]

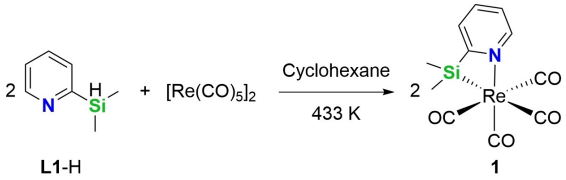

L1-H **1**

Scheme 1. Synthesis of the complex [Re(κ^2-*N*,*Si*-**L1**)(CO)$_4$] (**1**).

Some years later, Watts and collaborators reported the synthesis and characterization of rhodium- and iridium-(κ^2-*N*,*Si*)

[a] *Dr. M. Batuecas, Dr. A. Goméz-España, Prof. Dr. F. J. Fernández-Álvarez*
Departamento de Química Inorgánica – Instituto de Síntesis Química y Catálisis Homogénea (ISQCH)
Universidad de Zaragoza -CSIC
Facultad de Ciencias, Plaza de San Francisco, 50009, Zaragoza, Spain
E-mail: mbatuecas@unizar.es
paco@unizar.es
[b] *Dr. A. Goméz-España*
Centro de Investigación e Innovación Educativas (CIIE)
Universidad Pedagógica Nacional Francisco Morazán-UPNFM
Tegucigalpa, 11101, Honduras.

complexes with 8-quinolyldimethylsilyl based ligands (Scheme 2).[10] Thus, the reaction of 8-(dimethylsilyl)quinoline

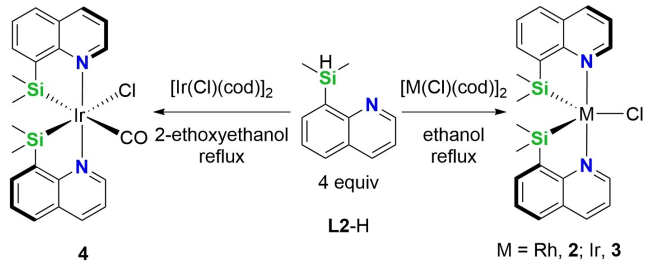

Scheme 2. Synthesis of complexes [M(Cl)(κ²-*N*,*Si*-**L2**)$_2$] (M = Rh, **2**; Ir, **3**) and [Ir(Cl)(κ²-*N*,*Si*-**L2**)$_2$(CO)] (**4**).

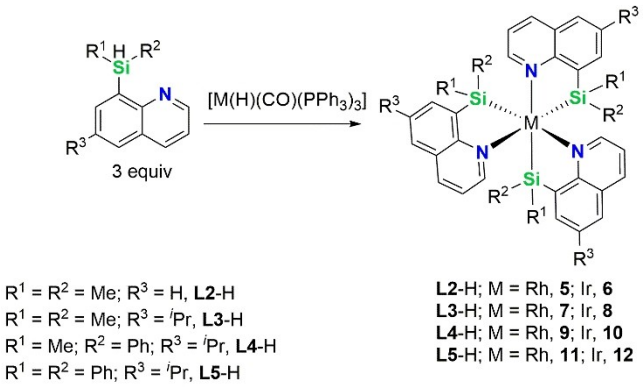

Scheme 3. Synthesis of complexes [M(κ²-*Si*,*N*-**Ln**)$_3$] (**Ln** = **L2**, **L3**, **L4** and **L5**).

with [{M(cod)}$_2$(μ-Cl)$_2$] (M = Rh or Ir; cod = 1,5-cyclooctadiene) in refluxing ethanol affords the corresponding species [M(Cl)(κ²-*N*,*Si*-**L2**)$_2$] (**L2** = (8-quinolyl)dimethylsilyl; M = Rh, **2**; Ir, **3**). The solvent matters, thus when the reaction with [{Ir(cod)}$_2$(μ-Cl)$_2$] was set up in refluxing 2-ethoxyethanol the octahedral Ir(III) complex [Ir(Cl)(κ²-*N*,*Si*-**L2**)$_2$(CO)] (**4**) was obtained.[10a]

The same group reported that using the complexes [M(H)(PPh$_3$)$_3$(CO)] (M = Rh, Ir) as metallic precursors and toluene as solvent, the coordination of three ligand units to generate the corresponding *fac*-[M(κ²-*N*,*Si*-**L2**)$_3$] (M = Rh, **5**; Ir, **6**) species takes place (Scheme 3).[10a,b] This methodology has been used successfully to prepare a number of *fac*-[M(κ²-*N*,*Si*-**Ln**)$_3$] species (**Ln** = **L3**, (6-isopropyl-8-quinolyl)dimethylsilyl, M = Rh, **7**; Ir, **8**; **Ln** = **L4**, (6-isopropyl-8-quinolyl)phenylmethylsilyl, M = Rh, **9**; Ir, **10**; and **Ln** = **L5** (6-isopropyl-8-quinolyl)diphenylsilyl, M = Rh, **11**; Ir, **12**), which stand out for their interesting optical properties.[10] The metal–Si bond distances in complexes **5** (2.278(1), 2.290(1) and 2.301(1) Å) and **6** (2.296(4), 2.301(4) and 2.305(4) Å)[10b] are shorter than should be expected for a Rh– or Ir–silyl bond.[2b,c,d]

Yoshizawa, Nishibayashi *et al.* reported in 2015 the synthesis of the related Co(III) species [Co(κ²-*N*,*Si*-**L6**)$_3$] (**13**) (**L6** = 2-(dimethylsilyl)methylpyridine) by reaction of [Co(H)(N$_2$)(PPh$_3$)$_3$] with the corresponding functionalized silane in THF at room temperature (r.t.). Complex **13** was characterized by ^{1}H and ^{13}C NMR spectroscopy and X-ray diffraction analysis, the Co–Si bond distances in **13** are in the range of 2.2311(8)–2.2424(9) Å (Scheme 4).[11]

María Batuecas received her degree in Chemistry at the University Complutense of Madrid. Then, she studied her PhD in Organometallic Chemistry in Zaragoza under the supervision of Prof. Esteruelas and Dr. García-Yebra. Upon graduating, she joined Prof. Larrosa group at the University of Manchester (MSCA fellowship). Following a postdoc with Prof. Fernández (Almeria), she returned to the UK as a postdoc in the Prof. Crimmin group. Currently, she is back at University of Zaragoza working in collaboration with Prof. Fernández-Alvarez as MSCA-Cofund fellow. Her research interest focuses on the design synthesis, and study of new transition-metal and main group complexes.

Alejandra Gómez-España is Associate Professor at the Centro de Investigación e Innovación Educativa of the Universidad Pedagogica Nacional Francisco Morazán -(UPNFM). She completed her master's degree (M.Sc.) in Educational Chemistry at the UPNFM in Tegucigalpa (Honduras) in 2017. In 2020, she moved to the University of Zaragoza (España) where she recieved the PhD degree in Chemistry in 2023 under the supevision of Prof. Fernander-Alvarez and Dr. Iglesias. Her PhD thesis was focused on the developmet of Rh and Ir catalysts with κ²-N,Si ligands.

Francisco J. Fernández-Álvarez is Professor Titular at the University of Zaragoza (España). He received his PhD in Chemistry at the University of Alcalá (Madrid, 1999) in Prof. Royo's group. He did postdoctoral stays at the Universities of Zurich (Prof. Berke) and Zaragoza (Prof. Esteruelas). He began his independent career at the University of Zaragoza (2011) in collaboration with Prof. Oro and Prof. Perez-Torrente. He has studied the chemistry of Rh and Ir complexes with tri- and bidentate organosilyl ligands and their potential as homogeneous catalysts for CO_2 and small molecules activation, field in which he is co-author of several publications.

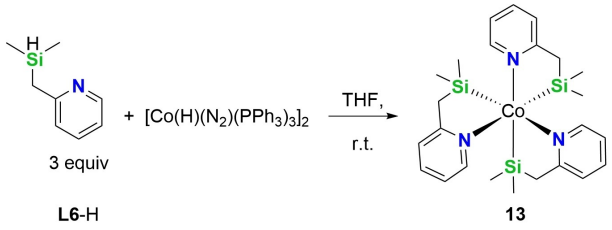

Scheme 4. Synthesis of the complex [Co(κ²-*N*,*Si*-**L6**)₃] (**13**).

Huertos *et al.* have been protagonists in the recent emergence of the chemistry of rhodium with 8-quinolyl based and related κ²-*N*,*Si* ligands,[12,13] focusing on the synthesis of unsaturated species and on the study of their catalytic applications. Thus, they recently prepared the 16-electron cationic species [Rh(κ²-*N*,*Si*-**L2**)₂(NCMe)][BAr$^F_4$] (**14**) (BAr$^F_4$ = tetrakis[3,5-bis(trifluoromethyl)phenyl]borate*)* by reaction of **2** with Na[BAr$^F_4$] in CH_2Cl_2 / acetonitrile. Compound **14** reacts with bipyridine to give the saturated cationic species [Rh(κ²-*N*,*Si*-**L2**)₂(bipy)][BAr$^F_4$] (**15**) (Scheme 5).[12]

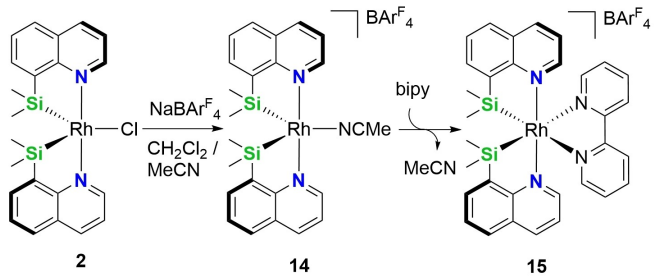

Scheme 5. Synthesis of the Rh-(κ²-*N*,*Si*) cationic species **14** and **15**.

Moreover, using this methodology, they were able to prepare the unsaturated 14-electron species [Rh(κ²-*N*,*Si*-**Ln**)₂][BAr$^F_4$] (**Ln** = **L7**, 8-(dimethylsilyl)-2-methylquinoline, **16**; **Ln** = **L8**, (9-phenyl-4-acridyl)dimethylsilyl, **17**) (Scheme 6).[12] NBO and QTAIM analysis of complexes **16** and **17**, revealed that agostic interactions Rh···H–C are present in both compounds. In addition, it should be mentioned that the Rh–Si bond distances in **2** (2.2571(6) Å; 2.2500(6) Å), **16** (2.2746(7) Å; 2.2654(8) Å) and **17** (2.2573(8) Å; 2.2498(8) Å) are shorter than should be expected for a Rh–silyl bond.[2b,c,d] Complexes **16** and **17** have proven to be highly effective catalysts for the selective hydrolysis of diphenylsilane.

Huertos *et al.* have also reported that using [Rh(Cl)(PPh₃)₃] as rhodium precursor it is possible to prepare Rh-(κ²-*N*,*Si*) complexes containing only one κ²-(*N*,*Si*) ligand. Thus, the reaction of 8-(dimethylsilyl)quinoline, 8-(dimethylsilyl)-2-methylquinoline and 4-(dimethylsilyl)-9-phenylacridine with [Rh(Cl)(PPh₃)₃] in CH_2Cl_2 affords the corresponding species [Rh(H)(Cl)(κ²-*N*,*Si*-**Ln**)₂(PPh₃)] (**Ln** = **L2**, **18**; **Ln** = **L7**, **19**; and **Ln** = **L8**, **20**), which react with Na[BAr$^F_4$] in CH_2Cl_2 to give the corresponding cationic species [Rh(H)(κ²-**Ln**)(PPh₃)₂][BAr$^F_4$] (**Ln** = **L2**, **21**; **Ln** = **L7**, **22**; and **Ln** = **L8**, **23**) (Scheme 7).[13] The Rh–Si bond distance in the neutral species **19** (2.2635(7) Å) is shorter than

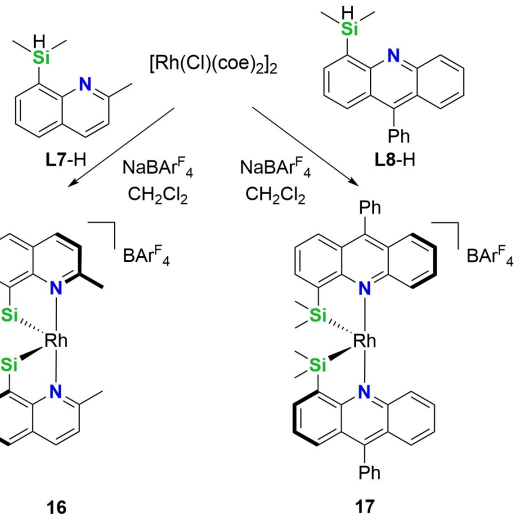

Scheme 6. Synthesis of the 14-electron unsaturated Rh-(κ²-*N*,*Si*) cationic species **16** and **17**.

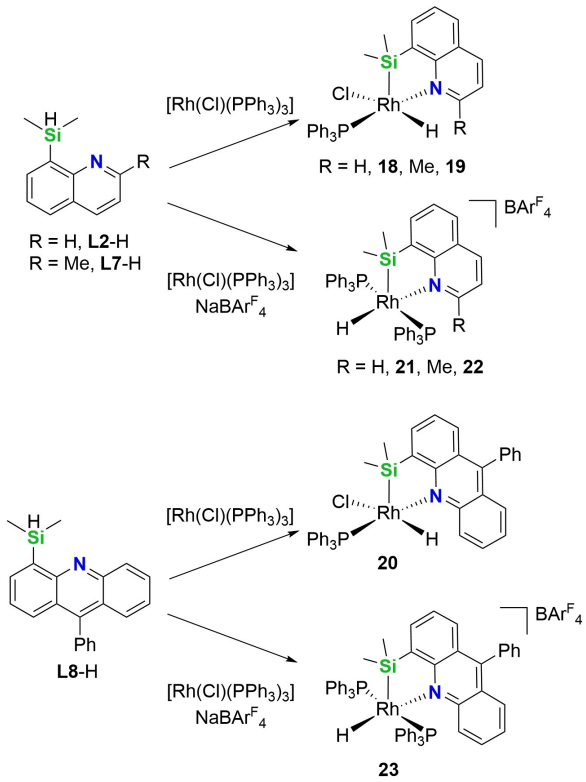

Scheme 7. Synthesis of the Rh-(κ²-*N*,*Si*) species **18**, **19**, **20**, **21**, **22** and **23**.

that found for **22** (2.2985(9) Å). The cationic species **21**, **22**, and **23** are active catalysts for the hydrosilylation of remote alkenes to give the corresponding lineal organosilane, the best catalytic

performance was achieved using complex **21** as catalyst precursor.[13]

Komuro, Hashimoto and collaborators have recently reported the synthesis of M-(κ^3-*N,N,Si*-**L9**) (M = Rh, Ir) complexes with the tridentate ligand 2-(ditertbutylsilyl)methyl-1,8-naphtyridine) (**L9**).[14] They have also reported the synthesis of rhodium and iridium complexes in which **L9** acts as bidentate κ^2-*N,Si* ligand.[15] Thus, the reaction of the proligand **L9**-H with [{Rh(coe)$_2$}$_2$(μ-Cl)$_2$] (coe = *cis*-cyclooctene) affords the dinuclear complex [{Rh(H)(κ^2-*N,Si*-**L9**)}$_2$(μ-Cl)$_2$] (**24**), which reacts with excess of BH_3-SMe_2 to afford the mononuclear BH_3 adduct [Rh(H)(Cl){κ^4-*Si,N,H,H*,-**L9**-(BH_3)}] (**25**) (Scheme 8).[15a] The Rh–Si

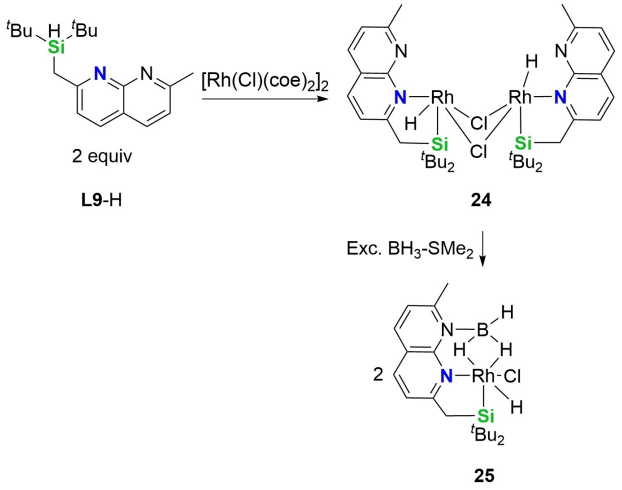

Scheme 8. Synthesis of the Rh-(κ^2-*N,Si*) complexes **24** and **25**.

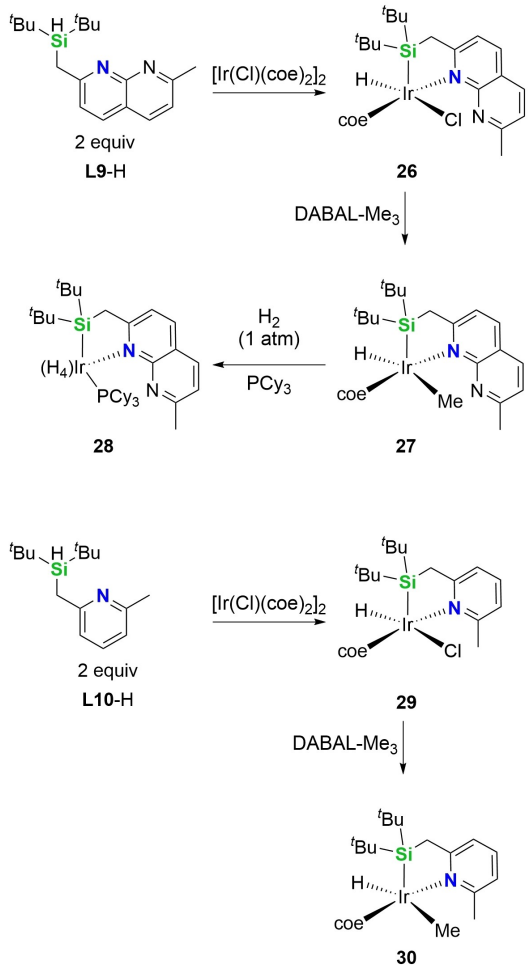

Scheme 9. Synthesis of the Ir-(κ^2-*N,Si*) **26**, **27**, **28**, **29** and **30**.

bond distances in **24** (2.2648(4) Å and in **25** (2.2990(8) Å) compare to those found for complexes **19** and **22**.

The proligand **L9**-H reacts with [{Ir(coe)$_2$}$_2$(μ-Cl)$_2$] to give the iridium(III) complex [Ir(H)(Cl)(κ^2-*N,Si*-**L9**)(coe)] (**26**), which reacts with DABAL-Me_3 (Bis(trimethylaluminum)-1,4-diazabicyclo[2.2.2]octane adduct, ($AlMe_3$)$_2$-DABCO) to afford the Ir-methyl complex [Ir(H)(CH_3)(κ^2-*N,Si*-**L9**)](coe)] (**27**). ^{1}H NMR studies of the reaction of **27** with H_2 (1 atm) and PCy_3 evidenced the formation of the Ir(V) tetrahydride [Ir(H_4)(κ^2-*N,Si*-**L9**)](PCy_3) (**28**), which was characterized in solution by means of multinuclear NMR spectroscopy (Scheme 9).[15b] Complexes **26** and **27** were also characterized by X-ray diffraction, the Ir–Si bond distances for these complexes are 2.3016(10) Å and 2.2887(14) Å, respectively.[15b] Same authors have also reported the synthesis of the related iridium(III) species [Ir(H)(Cl)(κ^2-*N,Si*-**L10**)(coe)] (**29**) and [Ir(H)(CH_3)(κ^2-*N,Si*-**L10**)(coe)] (**30**) (**L10** = 2-(ditertbutylsilyl)methyl-6-methyl-pyridine) (Scheme 9). The Ir-methyl derivatives **27** and **30** are effective catalytic precursors for hydrogenation of olefins. However, the activity of **27** is higher than that found for **30**, which proves the relevance of the nitrogen lone pair of **27** on the catalytic activity. Thus, the authors have proposed that in the case of **27**-catalyzed hydrogenation of alkenes, the H_2 activation could occur through a cooperative Lewis acid/base process between the nitrogen and the metal center.[15b]

Another type of *N,Si* bidentate ligands are those based on 2-pyridones. To the best of our knowledge, first examples of a TM-complex with a 2-pyridone based ligand were the iron species [Fe(η^5-C_5R_5)(κ^2-*N,Si*-**L11**)(CO)] (**L11** = (pyridine-2-yloxy)dimethysilyl; R = H, **31**; Me, **32**) reported by Tobita and collaborators.[16] The Fe-(κ^2-*N,Si*) complexes **31** and **32** where obtained by photolysis of the precursor [Fe(η^5-C_5R_5)(κ^1-Si-**L11**)($CO)_2$] or by irradiation of complex [Fe(η^5-C_5R_5)($CO)_2$($SiMe_3$)] in the presence of proligand **L11**-H (Scheme 10).[16]

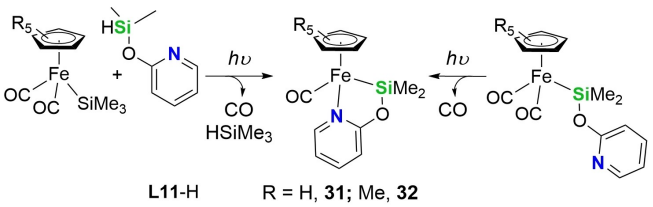

Scheme 10. Synthesis of the Fe-(κ^2-*N,Si*) complexes **31** and **32**.

Same group has also reported examples of Mo and W complexes with κ²-*N*,*Si* ligands. Compounds [M(η^5-C_5Me_5)(κ²-*N*,*Si*-**L12**)(CO)$_2$] (**L12** = (pyridine-2-yloxy)bisparatolylsilyl; M = Mo, **33**; W, **34**) were prepared by reaction of η^3-α-silabenzenyl species [M(η^5-C_5Me_5){κ³-(*Si*,*C*,*C*)-Si(*p*-Tol)$_3$}(CO)$_2$] (M = Mo, W) with 2-hydroxypyridine (Scheme 11).[17]

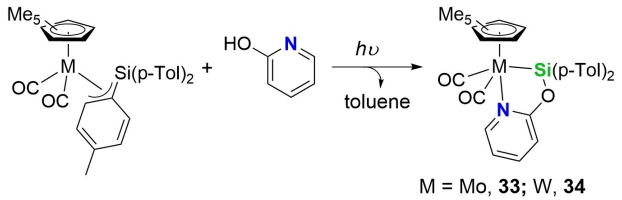

Scheme 11. Synthesis of the complexes Mo-(κ²-*N*,*Si*) (**33**) and Mo-(κ²-*N*,*Si*) (**34**).

Roper, Wright *et al.* reported the preparation of Ru-(κ²-*N*,*Si*) complexes by nucleophilic substitution reaction of the Si–Cl bond in [Ru(SiClPh$_2$)(κ²-S_2CNMe_2)(CO)(PPh$_3$)$_2$]. Thus, reaction of Ru-(κ²-S_2CNMe_2) precursor with 2-hydroxypyridine and 2-aminopyridine affords the corresponding species [Ru(κ²-*N*,*Si*-**L13**)(κ²-S_2CNMe_2)(CO)(PPh$_3$)] (**L13** = (pyridine-2-yloxy)bisphenylsilyl, **35**) and [Ru(κ²-*N*,*Si*-**L14**)(κ²-S_2CNMe_2)(CO)(PPh$_3$)] (**L14** = N-(diphenylsilyl)pyridine-2-amine, **36**), respectively (Scheme 12).[18]

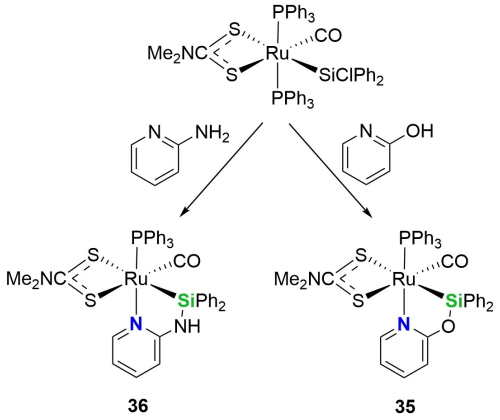

Scheme 12. Synthesis of the Ru-(κ²-*N*,*Si*) complexes **35** and **36**.

The Ru–Si bond distances found for **35** (2.3487(4) Å) and **36** (2.3400(7) Å) are in the expected range for Ru-silyl complexes.[2b,c,d]

Iridium complexes with 4-methylpyridin-2-yloxy-dimethylsilyl (**L15**),[19] 4-methylpyridin-2-yloxy-diisopropylsilyl (**L16**),[20] and 4-methylpyridin-2-yloxy-ditertbutylsilyl (**L17**)[21] ligands have been prepared by reaction of the corresponding pyridine-2-yloxy-silane derivative with [{Ir(coe)$_2$}$_2$(μ-Cl)$_2$]. The bulkiness of the substituents at the silicon atom of the κ²-*N*,*Si* ligand strongly influences the nature of the reaction products. Thus, in iridium(III) complexes with κ²-*N*,*Si*-**L15**[19] and κ²-*N*,*Si*-**L16**[20] ligands the coordination of two ligand units to the metal center to give the corresponding species [{Ir(κ²-*N*,*Si*-**L15**)$_2$}$_2$(μ-Cl)$_2$] (**37**)[19] or [Ir(Cl)(κ²-*N*,*Si*-**L16**)$_2$] (**38**)[20] respectively, is favored. However, when using **L17**-H proligand, which contains tertbutyl, instead of methyl or isopropyl substituents, the coordination of only one ligand unit to the metal center, to give the complex [Ir(H)(Cl)(κ²-*N*,*Si*-**L17**)(coe)] (**39**) is observed (Scheme 13).[21]

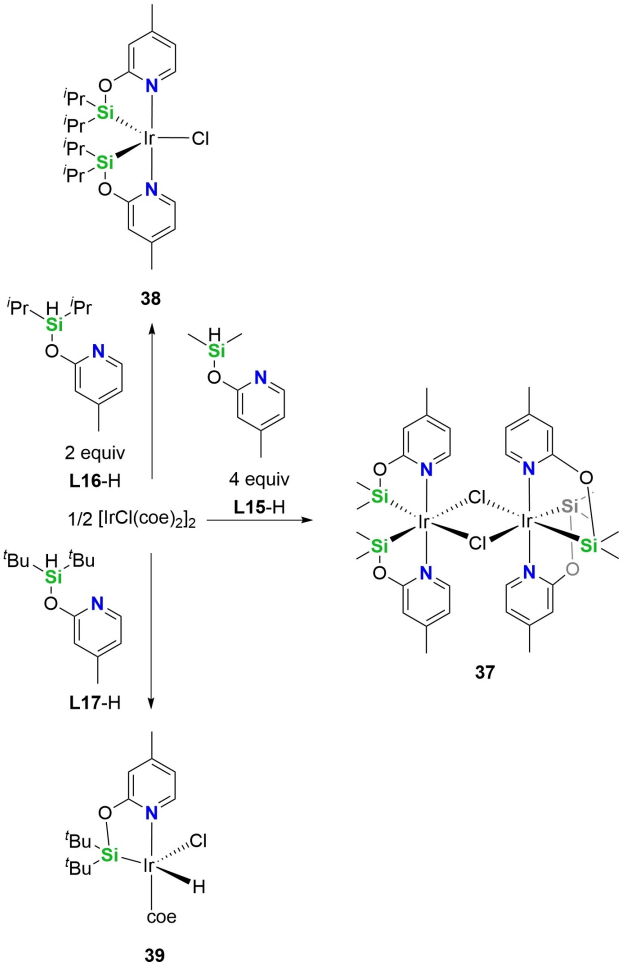

Scheme 13. Synthesis of the Ir-(κ²-*N*,*Si*) complexes **37**, **38** and **39**.

The reaction of **37** and/or **38** with one equivalent of Ag(O_2CCF_3) (AgTFA) quantitatively affords the corresponding iridium-trifluoroacetate derivative [Ir(κ²-O_2CCF_3)(κ²-*N*,*Si*-**L15**)$_2$] (**40**)[19] and [Ir(κ²-O_2CCF_3)(κ²-*N*,*Si*-**L16**)$_2$] (**41**).[20] The nature of the reaction product obtained from the reaction of **37** and/or **38** with Ag(OSO_2CF_3) (AgOTf) depends on the substituents at the silicon atom. Thus, while the reaction of **37** with one equivalent of AgOTf per iridium gives the dinuclear species [{Ir(κ²-*N*,*Si*-**L15**)$_2$}$_2$(μ-OTf)$_2$] (**42**),[22] under the same conditions the reaction of **38** with AgOTf affords the mononuclear complex [Ir(κ¹-*O*-OTf)(κ²-*N*,*Si*-**L15**)$_2$] (**43**) (Scheme 14).[20] To the best of our knowledge, complex **42** is the first example of an iridium species with triflate ligands acting as bridge.

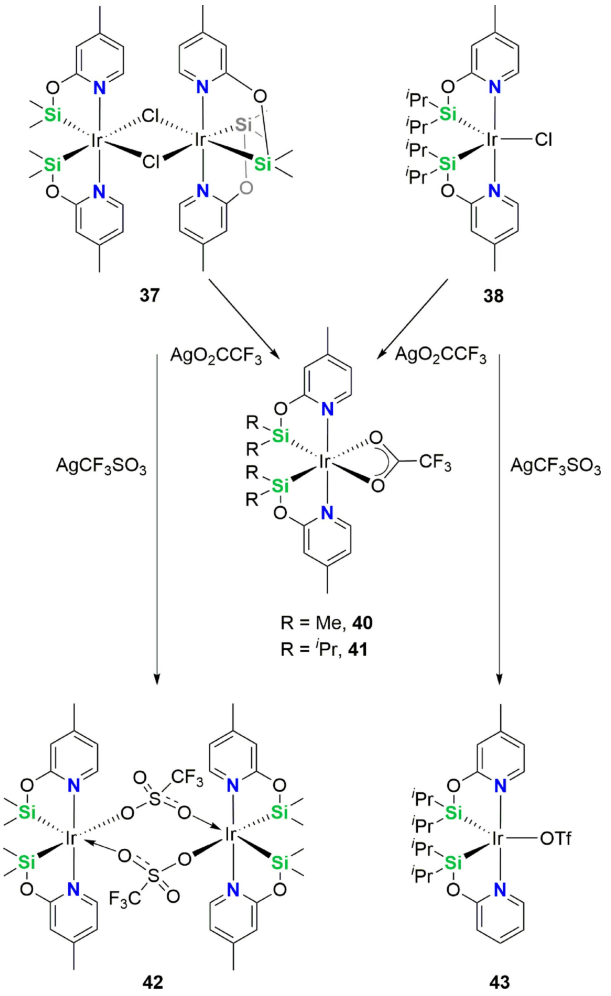

Scheme 14. Synthesis of the Ir-(κ^2-*N*,*Si*) complexes **40**, **41**, **42** and **43**.

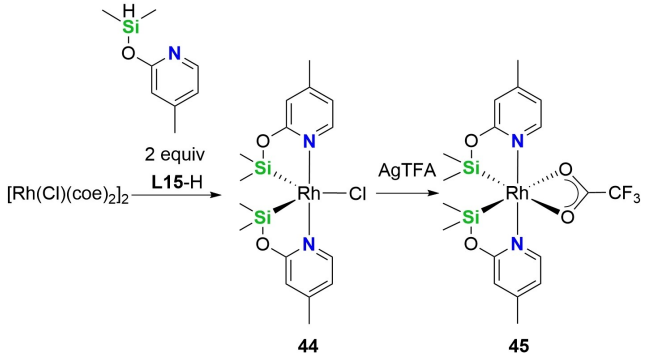

Scheme 15. Synthesis of the Ir-(κ^2-*N*,*Si*) complexes **44** and **45**.

The iridium species **40** has proven to be an effective catalysts for the selective reduction of CO_2 with silanes to the formate (4 bar of CO_2) or methoxy (1 bar of CO_2) level.[19] Moreover, when the catalytic system **40**/$B(C_6F_5)_3$ was used as catalyst for the reaction of CO_2 (1 bar) with hydrosilanes, the corresponding bis(silyl)acetal, $CH_2(OSiR_3)_2$, was selectively obtained.[23] The ancillary ligand also plays a key role in the selectivity of these catalytic processes, thus when the triflate derivative **42** was used as catalyst for the reduction of CO_2 with hydrosilanes mixtures of the corresponding silylformate, methoxysilane and methylsilylcarbonate (MeO–C(O)-$OSiR_3$) were obtained.[22] It should be noted that the Ir-(κ^2-*N*,*Si*) species **40** has a better catalytic performance than related Ir-*fac*-(κ^3-*N*,*Si*,*N*) catalysts. The lower activity of Ir-*fac*-(κ^3-*N*,*Si*,*N*) species has been attributed to the steric hindrance and rigidity of the tridentate ligands.[24]

The proligand **L15**-H has also been succesfully used to prepare rhodium complexes. Thus, the reaction of **L15**-H with [{Rh(coe)$_2$}$_2$(μ-Cl)$_2$] affords the mononuclear rhodium(III) species [Rh(Cl)(κ^2-*N*,*Si*-**L15**)$_2$] (**44**), related to **2**, which reacts with AgTFA to give the pseudoactahedral complex [Rh(κ^2-O_2CCF_3)(κ^2-*N*,*Si*-**L15**)$_2$] (**45**) (Scheme 15).[25] Differently to **40**, the rhodium derivative **45** has shown no activity as CO_2 hydrosillyation catalyst under the same reaction conditions. However, **45** is an effective catalyst for the formation of silylcarbamates from the reaction of CO_2 with secondary amines and hydrosilanes.[25]

Complex [Ir(H)(Cl)(κ^2-*N*,*Si*-**L17**)(coe)] (**39**) reacts with AgOTf to afford the triflate derivative [Ir(H)(κ^1-*O*-OTf)(κ^2-*N*,*Si*-**L17**)(coe)] (**46**) (Scheme 16). Both species **39** and **46** are active catalysts for

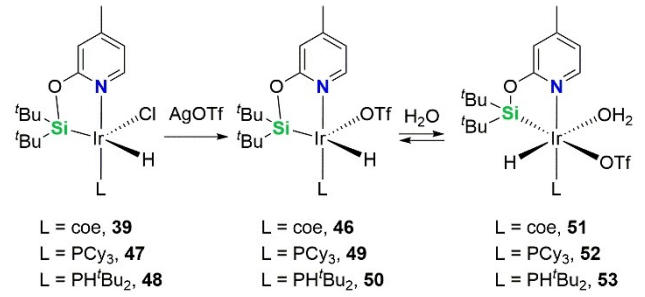

Scheme 16. Reaction sequence from **39**, **47** and **48** towards the aquo complexes **51**, **52** and **53**.

the reduction of formamides to the corresponding methylamine with hydrosilanes. Moreover, using **39** as catalyst, the reaction proceeds step by step, making it possible to obtain selectively the corresponding *O*-silylatedhemiaminal.[21] The reaction of **39** with PCy_3 and/or PH^tBu_2 quantitatively affords the species [Ir(H)(Cl)(κ^2-*N*,*Si*-**L17**))(L)] (L = PCy_3, **47**; PH^tBu_2, **48**), which reacts with AgOTf to give the corresponding triflate derivative [Ir(H)(OTf)(κ^2-*N*,*Si*-**L17**)(L)] (L = PCy_3, **49**; PH^tBu_2, **50**). In presence of H_2O the 16-electron unsaturated iridium triflate derivatives **46**, **49** and **50** are in equilibrium with the corresponding water aduct [Ir(H)(OTf)(κ^2-*N*,*Si*-**L17**)(L)(OH_2)] (L = coe, **51**; PCy_3, **52**; PH^tBu_2, **53**) (Scheme 16), which were characterized in solution by means of NMR spectroscopy and by X-ray diffraction methods.[26] These results show that the Ir–Si bond in species **48**, **49** and **50** is stable in the presence of moisture. Indeed, hydrolysis was only observed in the presence of an external base (NEt_3). Complexes **46** and **47** have proven to be selective

catalysts for the hydrolysis of $HSiMe(OSiMe_3)_2$ to give the corresponding hydroxysilane $HOSiMe(OSiMe_3)_2$.[26]

Complex **39** reacts with 4,4′-dimethyl-2,2′-bipyridine (bipy^{Me2}) in toluene at 353 K to give the 18-electron saturated species [Ir(H)(Cl)(κ^2-*N*,*Si*-**L17**)(bipy^{Me2})] (**54**), which reacts with AgOTf to afford the triflate derivative [Ir(H)(OTf)(κ^2-*N*,*Si*-**L17**)(bipy^{Me2})] (**55**) (Scheme 17).[27] Complex **55** has been found to be

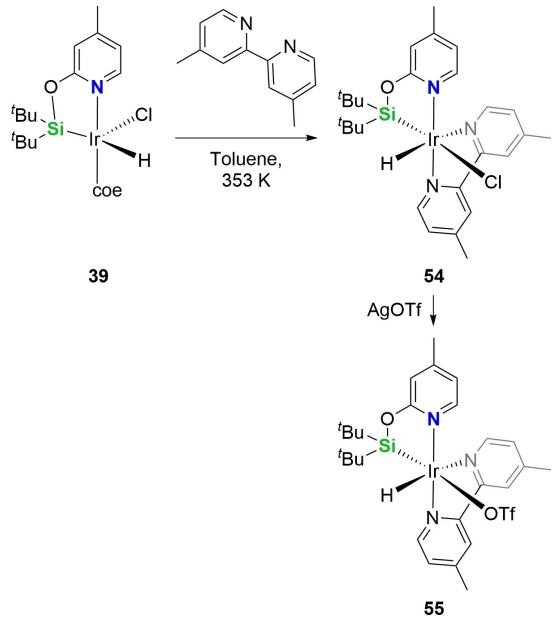

Scheme 17. Synthesis of the Ir-(κ^2-*N*,*Si*) complexes **54** and **55**.

an effective catalyst for the selective solventless dehydrogenation of formic acid,[27] its activity being slightly higher than that found for **40**.[28]

The rhodium species [Rh(H)(Cl)(κ^2-*N*,*Si*-**L17**)(L)] (L = PCy_3, **56**; PH^tBu_2, **57**) related to the iridium derivatives **47** and **48**, respectively, were prepared by reaction of [{Rh(coe)$_2$}$_2$(μ-Cl)$_2$] with one equivalent of the proligand **L17**-H per rhodium in the presence of stoichiometric amounts of PCy_3 (or PH^tBu_2) at 273 K. Treatment of toluene solutions of **56** (or **57**) with one equivalent of AgOTf affords the corresponding compounds [Rh(H)(OTf)(κ^2-*N*,*Si*-**L17**)(L)] (L = PCy_3, **58**; PH^tBu_2, **59**) (Scheme 18).[29]

Complexes **56–59** have proven to be effective catalyst for the selective hydrogenation of alkenes to alkanes. The best catalytic performance has been obtained when using the rhodium-triflate derivative **58** as catalyst at 353 K, which allows the quantitative and selective formation of the corresponding alkane in all the studied cases. It should be noted that the related iridium species **49**, although it is also active as alkene hydrogenation catalysts shows a poorer catalytic performance.[29]

Reaction of the proligand *N*-(dimethylsilyl)-*N*-methylpyridin-2-amine (**L18**-H) with [Fe(PMe$_3$)$_4$] has been successfully used to prepare the iron(II) complex [Fe(H)(κ^2-*N*,*Si*-**L18**)(PMe$_3$)$_3$] (**60**), which by reaction with alkyl halides (MeI or EtBr) affords the

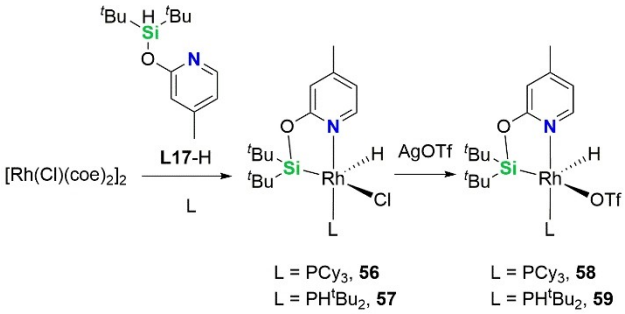

Scheme 18. Synthesis of the Rh-(κ^2-*N*,*Si*) complexes **56**, **57**, **58** and **59**.

corresponding substitution product [Fe(X)(κ^2-*N*,*Si*-**L18**)(PMe$_3$)$_3$] (X = I, **61**; Br, **62**). The Fe–H complex **60** reacts with CO_2 and phenylisocianate to give the corresponding insertion products [Fe(κ^2-O_2CH)(κ^2-*N*,*Si*-**L18**)(PMe$_3$)$_2$] (**63**) and [Fe(κ^2-*N*,*O*-PhNCHO)(κ^2-*N*,*Si*-**L18**)(PMe$_3$)$_2$] (**64**). The Fe–H bond of compound **60** reacts with acetylacetone (Hacac) to produce H_2 and complex [Fe(acac)(κ^2-*N*,*Si*-**L18**)(PMe$_3$)$_2$] (**65**) (Scheme 19).[30]

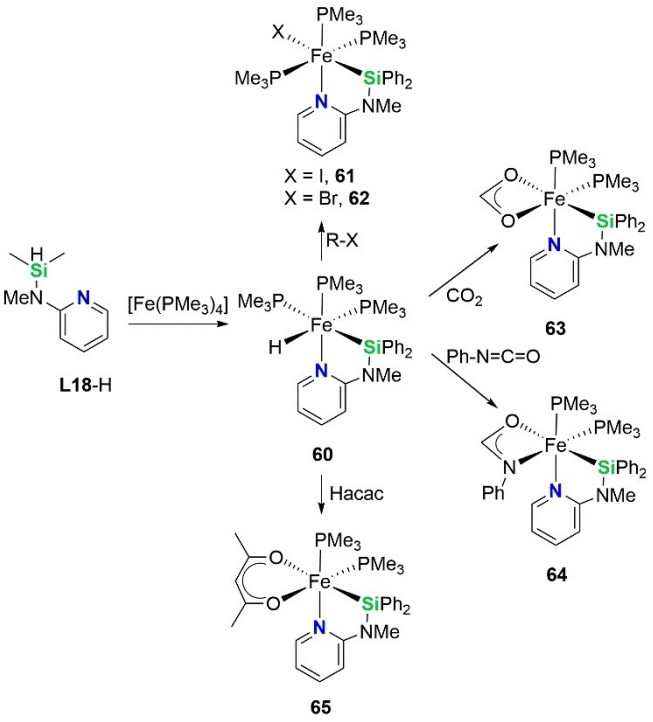

Scheme 19. Synthesis of the Fe-(κ^2-*N*,*Si*) complexes **60–65**.

The addition of the proligand **L18**-H to the Ru(0) complex [Ru(η^4-C_8H_{12})(η^6-C_8H_{10})] has been the entrance door to the chemistry of ruthenium with the κ^2-*N*,*Si*-**L18** ligand. The reaction of [Ru(η^4-C_8H_{12})(η^6-C_8H_{10})] with one equivalent of **L18**-H gives the ruthenium(II) complex [Ru(κ^2-*N*,*Si*-**L18**)(η^4-C_8H_{12})(η^3-C_8H_{11})] (**66**), which reacts with excess of **L18**-H at 333 K to give the species [Ru(H)(κ^2-*N*,*Si*-**L18**)$_3$] (**67**). Complex **67** can be also obtained by reaction of [Ru(η^4-C_8H_{12})(η^6-C_8H_{10})] with excess of

L18-H at 333 K. The reaction of **66** with one equivalent of **L18**-H under H_2 (3 bar) atmosphere give the dinuclear complex [{Ru-(H)(κ^2-*N*,*Si*-**L18**)$_2$}(μ-H)$_2$] (**68**), which by reaction with 2.5 equivalents of **L18**-H at 323 K gives **67** (Scheme 20).[31]

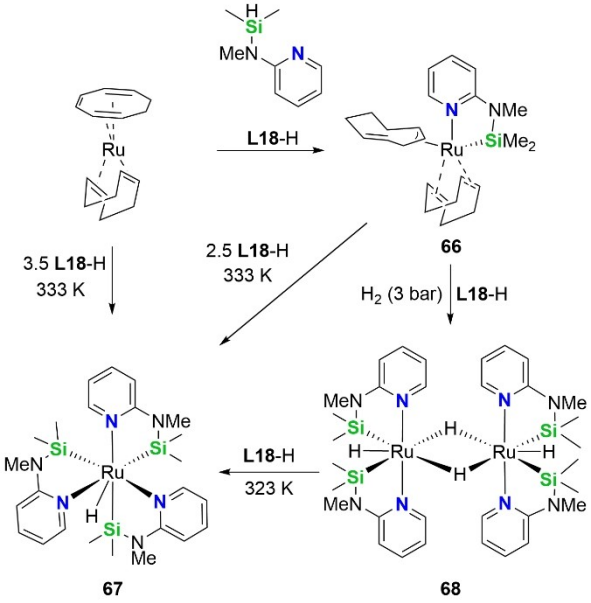

Scheme 20. Synthesis of the Ru-(κ^2-*N*,*Si*) complexes **66**, **67** and **68**.

2.2. Transition Metal Complexes with κ^2-*P*,*Si* Ligands

Phosphanosilyl moieties are usually bounded to the metal center as a bidentate chelate-type ligand. This chelate effect increases stability of the TM-(κ^2-*P*,*Si*) complexes avoiding the elimination of silyl groups from the metal center *via* reductive elimination, nucleophilic attack at the silicon atom, insertion or σ-bond metathesis.[32]

To the best of our knowledge, the first examples of TM-complexes with monoanionic κ^2-phosphanosilyl ligands ($X_2SiCH_2CH_2P(CH_3)_2$, X = CH_3, **L19**; X = Cl, **L20**), were reported by Grobe and Walter in 1977.[33] Thus, the Mn-(κ^2-*P*,*Si*) complexes [Mn(κ^2-*P*,*Si*-{$SiX_2CH_2CH_2P(CH_3)_2$})$(CO)_4$] (X = CH_3 **69**; Cl, **70**) were successfully synthetized by reaction of Na[$Mn(CO_5)$] and [Mn-(H)$(CO)_5$] with the corresponding proligand to afford the silyl complexes [Mn(κ^1-*Si*-{$SiX_2CH_2CH_2P(CH_3)_2$})$(CO)_5$], which by photochemical activation of a Mn–CO bond evolve to the corresponding complex **69** or **70** (Scheme 21).[33]

It was not until 1981 that a systematic approach to prepare [Pt(κ^2-*P*,*Si*-$SiR^1R^2CH_2CH_2PPh_2$)] (R^1 = R^2 = Me, **71 a**; R^1 = R^2 = Ph, **71 b**; R^1 = Me, R^2 = Ph, **71 c**; R^1 = H, R^2 = Me, **71 d**; R^1 = H, R^2 = Ph, **71 e**) species was reported by Stobart *et al.*[34] This family of Pt-(κ^2-*P*,*Si*) complexes was easily obtained by oxidative addition of the Si–H bond of the corresponding $PPh_2CH_2CH_2SiHR^1R^2$ proligand to [Pt$(cod)_2$] (Scheme 22). Since these pioneering results the chemistry of TM-(κ^2-*P*,*Si*) complexes developed significantly in subsequent decades. In this regards Okazaki and coworkers

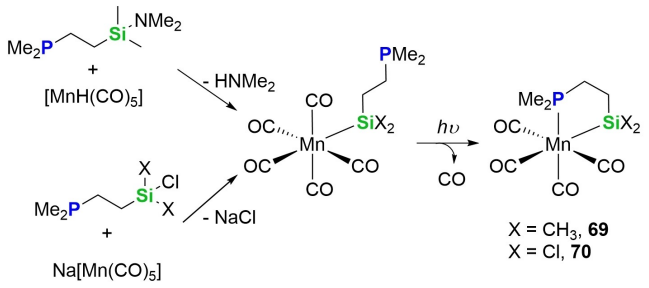

Scheme 21. Synthesis of [Mn(κ^2-*P*,*Si*-{$SiX_2CH_2CH_2P(CH_3)_2$})$(CO)_4$] (X = CH_3 **69**; Cl, **70**).

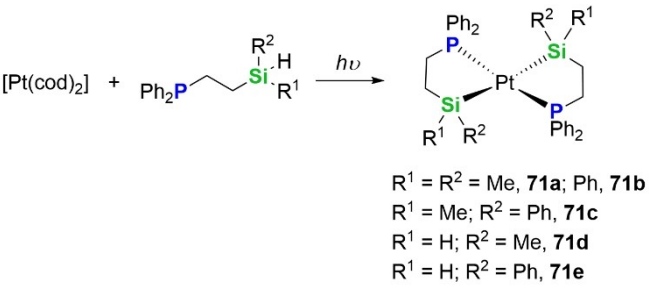

Scheme 22. Synthesis of Pt-(κ^2-*P*,*Si*) complexes **71 a-e**.

published a review that describes the chemistry of TM-(κ^2-*P*,*Si*) complexes published until 2002.[6] Therefore, our present revision focuses attention on results published from 2002 onwards.

Sunada and coworkers reported the reaction of [Pd-($CN^tBu)_2$]$_3$ with the disilane $(Ph_2PCH_2)Ph_2Si$-$SiPh_2(CH_2PPh_2)$ (**L21**)$_2$ to form a triangular palladium cluster.[35] Thus, reaction of 4 / 3 equivalents of [Pd($CN^tBu)_2$]$_3$ with (**L21**)$_2$ in toluene at 353 K led to the formation of a trinuclear palladium cluster (**72**) with two κ^2-*P*,*Si* chelating ligands linked by a $-CH_2$-Ph_2Si-CH_2- backbone generated *via* a skeletal rearrangement of the disilane framework (Scheme 23).

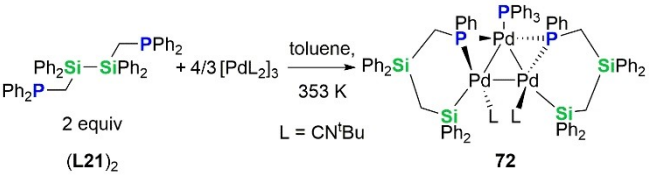

Scheme 23. Synthesis of trinuclear palladium cluster **72**.

Sunada group also has found that disilanes (**L21**)$_2$ and (**L22**)$_2$ react with [{Ir(cod)}$_2$(μ-Cl)$_2$] to give the 16-electron unsaturated complexes [Ir(Cl)(κ^2-*P*,*Si*-$SiR_2CH_2PPh_2$)$_2$] (R = Ph, **73**; R = Me, **74**) (Scheme 24).[36] The Ir–Si bond distances found in **74** are in expected range for Ir–silyl bonds (Table 2). Complexes **73** and **74** are active catalysts for the (*E*)-selective semi-hydrogenation of alkynes. The performance of these iridium species depends on the substituents on the silicon atoms, being

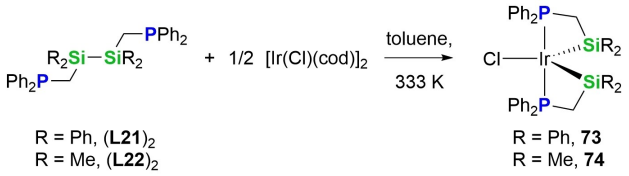

Scheme 24. Synthesis of Ir-(κ^2-*P*,*Si*) complexes **73** and **74**.

74, with methyl substituent more active and selective than **73**.[36]

Sola *et al.* reported the slow transformation of [Ir-(H)$_2$(biPSiF)(NCMe)$_2$]BF$_4$ (biPSiF = κ^2-*P*,*Si*-FSi(Me){(CH$_2$)$_3$PPh$_2$}$_2$) into the Ir-(κ^2-*P*,*Si*) complex [Ir{κ^2-*P*,*Si*-**L23**}(κ^2-*C*,*P*-CH$_2$CH$_2$CH$_2$PPh$_2$)(NCMe)$_2$]BF$_4$ (**75**), (**L23** = SiF(Me)CH$_2$CH$_2$CH$_2$PPh$_2$) (Scheme 25). The Ir–Si bond distance in

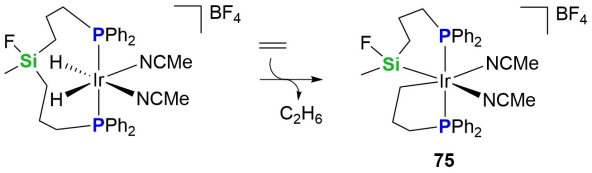

Scheme 25. Synthesis of the Ir-(κ^2-*P*,*Si*) complex **75**.

75 (2.3233(18) Å) is in the range of Ir–silyl bond distances. The formation of **75** can be described as a H$_2$ loss followed by Si–C bond activation. This assumption is supported by the fact that reaction times decrease significantly by adding a hydrogen acceptor as ethylene and demonstrates that the silicon atom at the polydentate ligand biPSi remains a reactive site.[37]

Le Floch, Sabo-Etienne and collaborators have reported the reaction of the Ru(II) complex [RuH$_2$(H$_2$)$_2$(PCy$_3$)$_2$] with three equivalents of the proligand PPh$_2$CH$_2$OSiMe$_2$H (**L24**-H), which results in the coordination of three ligands units and the substitution of the two PCy$_3$ and two H$_2$ molecules. The product of this reaction has been characterized by means of ^{1}H, ^{29}Si NMR and theoretical calculations as an equilibrium between the ruthenium(IV) species [Ru(H)$_2$(κ^2-*P*,*Si*-**L24**)$_2$(κ^1-P-**L24**-H)] (**76a**) and the ruthenium(II) complex [Ru(H)(κ^2-*P*,*Si*-**L24**)(κ^2-*P*,*Si*-*H*,-**L24**-H)(κ^1-*P*-**L24**-H)] (**76b**) and (Scheme 26).[38]

Ko, Kang and collaborators reported in 2004 the formation of stable *trans*-bis(κ^2-*P*,*Si*-chelate)metal complexes, using the (phosphinoalkyl)silane proligands **L25a**-H and **L25b**-H (Scheme 27) with a two-carbon skeleton connecting the silicon and phosphorus atoms that is part of a bulky *o*-carboranyl unit.[39] Reaction of the coordinatively unsaturated group 10 metal complex [Pt(PPh$_3$)$_2$(C$_2$H$_4$)] with **L25a**-H and/or **L25b**-H gave the corresponding metal complex [Pt{κ^2-*P*,*Si*-**Ln**}$_2$] (**Ln** = **L25a**, **77a**; **Ln** = **L25b**, **77b**) *via* chelate-assisted oxidative addition of the Si–H bond at palladium or platinum and subsequent release of H$_2$ (Scheme 27). The *trans*-complexes, **77a** and **77b**, can be isomerized to the corresponding *cis* species **78a** and **78b**, respectively, by thermal treatment

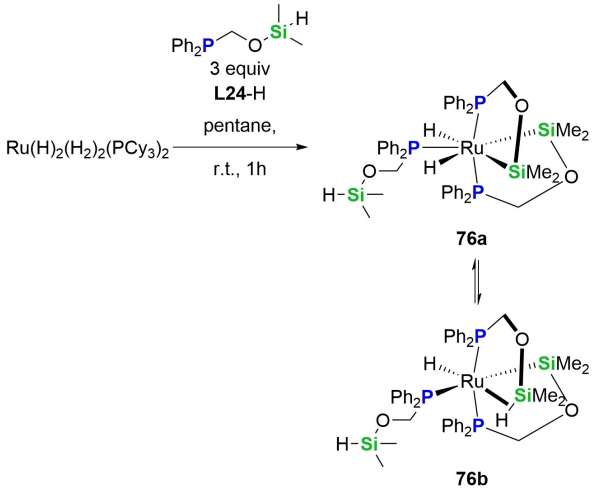

Scheme 26. Synthesis of **76** represented by two arrested structures (**76a** and **76b**).

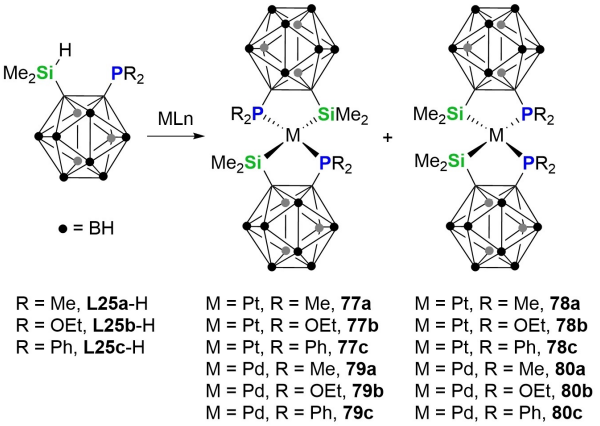

L25-H	MLn	M(**L25**)$_2$	ratio
L25a-H	[Pt(PPh$_3$)$_2$(C$_2$H$_4$)]	**77a**	-
L25b-H	[Pt(PPh$_3$)$_2$(C$_2$H$_4$)]	**77b**	-
L25a-H	[Pt(cod)$_2$]	**77a**, **78a**	2:1
L25b-H	[Pt(cod)$_2$]	**77b**, **78b**	1:1
L25c-H	[Pt(cod)$_2$]	**77c**, **78c**	1:6
L25a-H	[Pd$_2$(dba)$_3$]	**79a**, **80a**	2:1
L25b-H	[Pd$_2$(dba)$_3$]	**80b**	-
L25c-H	[Pd$_2$(dba)$_3$]	**80c**	-

Scheme 27. Reactivity of the phosphinoalkylsilanes **L25a**-H, **L25b**-H and **L25c**-H with metallic precursors (ML$_n$ = [Pt(PPh$_3$)$_2$(C$_2$H$_4$)], [Pt(cod)$_2$] and [Pd$_2$(dba)$_3$]).

(383 K) of their toluene solutions in the presence of an activated acetylene such as dimethyl acetylenedicarboxylate (DMAD).[39]

The *trans*/*cis* disposition of the ligand in the reaction product depends on the nature of the metallic precursor. Thus, when [Pt(cod)$_2$] was used as precursor, instead of [Pt-(PPh$_3$)$_2$(C$_2$H$_4$)], mixtures of *trans*/*cis* isomers in different ratios were obtained (Scheme 27). The palladium precursor [Pd$_2$(dba)$_3$] (dba = dibenzylideneacetone) reacts with **L25a**-H to give a mixture of complexes **79a** and **80a** in a ratio of 2:1,

respectively. However, the reaction of $[Pd_2(dba)_3]$ with **L25b**-H or **L25c**-H is selective to the formation of the corresponding *cis* isomer, **80 b** (65 %) or **80 c** (60 %), respectively. These results indicate that the stereoselectivity of the reaction depends on the electronic and steric characteristics of the ligands around the metal center.[39]

Interestingly, the reaction of $[Pt(PPh_3)_2(C_2H_4)]$ with **L25c**-H results in the mono(chelate) complex [Pt(H)(κ²-*P*,*Si*-**L25c**)(PPh_3)] (**81**), and the formation of the bis(chelate) species **77 c** or **78 c** was not observed. In the same way, $[Pt(cod)_2]$ reacts with **L25c**-H in the presence of the bulky ancillary *o*-carboranylphosphine ligand (Cab)PPh_2 to provide the sterically encumbered complex [Pt(H)(κ²-*P*,*Si*-**L25c**){κ¹-*P*-(Cab)PPh_2}] (**82**) (Scheme 28).[39]

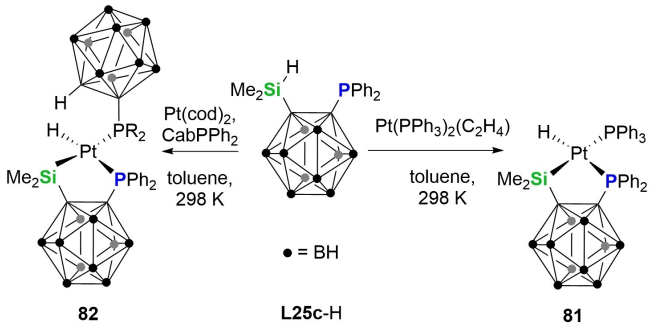

Scheme 28. Synthesis of the Ir-(κ²-*P*,*Si*) complexes **81** and **82**.

The *ortho*-silylated triphenylphosphine fragment κ²(*P*,*Si*)-$SiMe_2C_6H_4PPh_2$ (**L26**) can act as a ligand with a variety of TM. To the best of our knowledge, the first example of a TM-complex with this type of ligands was reported by Roper *et al.* in 1990. They obseved that the reaction of $[Os(H)(Cl)(CO)(PPh_3)_2]$ with $Hg(SiMe_3)_2$ did not afford the expected product, $[Os(SiMe_3)Cl(CO)(PPh_3)_2]$, but the complex [Os(κ²-*P*,*Si*-**L26**)(κ²-*C*,*P*-$C_6H_4PPh_2$)(CO)(PPh_3)] (**83**) was obtained in good yield (Scheme 29).[40] Some years later, a synthetic approach was

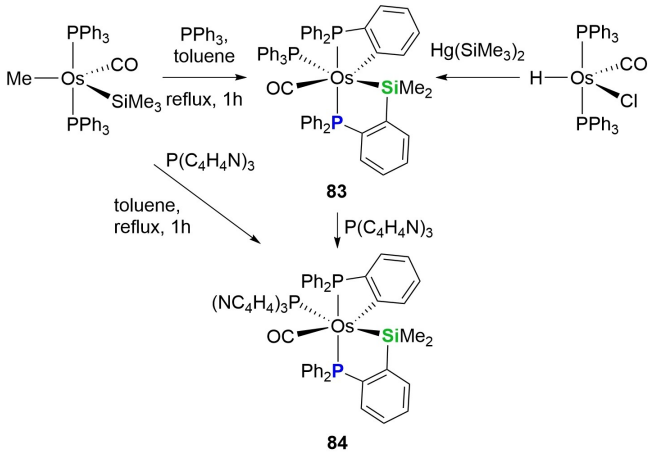

Scheme 29. Synthesis of the Os-(κ²-*P*,*Si*) complexes **83** and **84**.

published by the same group. Thus, refluxing toluene solutions of $[Os(SiMe_3)(Me)(CO)(PPh_3)_2]$ in the presence of PPh_3 results in the formation of complex **83**, which was isolated as colourless crystalline solid in 50 % yield.[41] An analogous compound [Os(κ²-*P*,*Si*-**L26**)(κ²-*C*,*P*-$C_6H_4PPh_2$)(CO)($P(C_4H_4N)_3$)] (**84**) was formed by thermal reaction of $[Os(SiMe_3)(Me)(CO)(PPh_3)_2]$ in the presence of tris(*N*-pyrrolyl)phosphine ($P(C_4H_4N)_3$) instead of triphenylphosphine (Scheme 29). The Os–Si bond distances in complexes **83** (2.4716(13) Å) and **84** (2.5110(8) Å) are longer than usual (around 2.45 Å),[41] but they are still in the Os–silyl bond distance range.[2b,c,d]

The formation of complexes **83** and **84** was postulated to occur through a dimethylsilylene intermediate arising from a migration of a methyl group from the trimethylsilyl group to osmium.[41] This assumption is based on a study previously reported by Tobita, Ogino and collaborators[42] in which the same *ortho*-silylated ligand κ²-*Si*,*P*-$SiMe_2C_6H_4PPh_2$ (**L26**) is formed in the thermal reaction of the base-stabilised silylene-triphenylphosphine ruthenium(II) complex [Ru(η^5-C_5H_5)(Ph_3P)-{$SiMe_2$·O(Me)·$SiMe_2$}] in the presence of different two-electron donor ligands to give the corresponding species [Ru(η^5-C_5H_5)(κ²-*P*,*Si*-**L26**)L] (L = PPh_3, **85 a**; L = PMe_3, **85 b**; L = PEt_3, **85 c**; L = $P(OMe)_3$, **85 d**; L = CN^tBu, **85 e**) (Scheme 30). The proposed

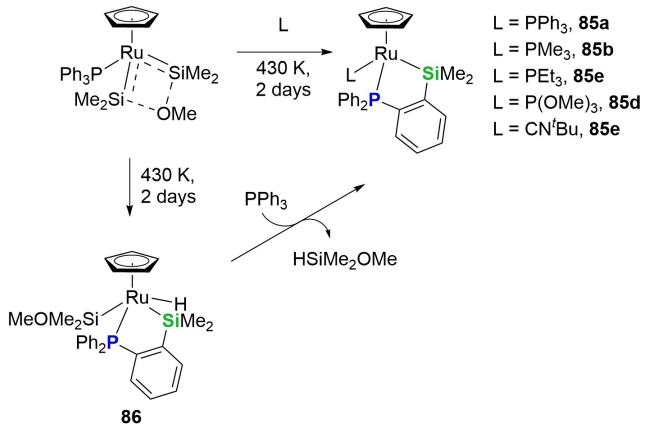

Scheme 30. Synthesis of the Ru-(κ²-*P*,*Si*) complexes **85 a**-**e** and **86**.

mechanism implies a C–H bond activation of a phenyl group by the Ru=Si double bond. To the best of our knowledge, this was the first example of a C–H bond activation assisted by a silylene complex. When a toluene solution of [Ru(η^5-C_5H_5)(Ph_3P)-{$SiMe_2$·O(Me)·$SiMe_2$}] was heated in the absence of a ligand a *ortho*-silylated ruthenium(IV) complex [Ru(η^5-C_5H_5)(H)(κ²-*P*,*Si*-**L26**)($SiMe_2OMe$)] (**86**) is formed. Complex **86** evolves to **85 a**, by reductive elimination of $HSiMe_2(MeO)$, when was heated in the presence of PPh_3, which suggests that **86** is an intermediate for the formation of complexes **85 a**-**e** (Scheme 30).[42]

In 2017, Sun and coworkers reported the synthesis of cobalt complexes bearing the κ²-(*P*,*Si*)-**L26** ligand.[43] The reaction of the proligand *o*-$HSi(Me)_2(PPh_2)C_6H_4$ (**L26**-H) with $[Co(Me)(PMe_3)_3]$ led to formation of the Co(I)-silyl complex [Co(κ²-*P*,*Si*-**L26**)(PMe_3)$_3$] (**87**). On the other hand, the reaction of **L26**-H with

[Co(Cl)(PMe$_3$)$_3$] gave the Co(III) species [Co(H)(Cl)(κ^2-*P*,*Si*-**L26**)(PMe$_3$)$_2$] (**88**). They also proved that the Co(III) complex **88** can be reduced with a strong base such as MeLi to give **87** in the presence of PPh$_3$ (Scheme 31).[43] The silyl [*P*,*Si*]-chelate

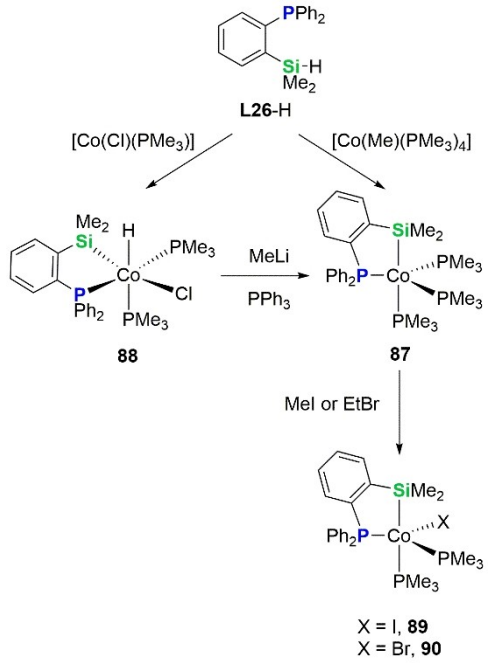

Scheme 31. Synthesis of the Co-(κ^2-*P*,*Si*) complexes **87**, **88**, **89** and **90**.

cobalt hydride **88** is catalytically more active for Kumada coupling reactions of aryl chlorides or aryl bromides with Grignard reagents than the related tridentate Co-(κ^3-*P*$_2$,*Si*)[44] and tetradentate Co-(κ^4-*P*$_3$,*Si*)[45] cobalt hydride derivatives.

Same authors reported reaction of **87** with one equivalent MeI or EtBr to afford the corresponding Co(II) complex [Co-(X)(κ^2-*P*,*Si*-**L26**)(PMe$_3$)$_2$] (X = I, **89**; Br, **90**). The Co–Si bond distances in **87** (Co(I); 2.3353(5) Å) and **89** (Co(II); 2.3368(9) Å) are longer than the Co–Si bond distance in the Co(III) complex **88** (2.2735(10) Å),[43] all of them in the Co–silyl range (Scheme 31).[2b,c,d]

Few years after, same group synthetized the iron silyl hydride complex [Fe(H)(κ^2-*P*,*Si*-**L26**)(PMe$_3$)$_3$] (**91**) by reaction of **L26**-H with Fe(PMe$_3$)$_4$.[46] The proposed mechanism for the formation of **91** involves the displacement of one PMe$_3$ ligand to give the intermediate [Fe(κ^1-*P*-**L26**-H)(PMe$_3$)$_3$] (**91-I**), followed by coordination of the Si–H bond to the metal center accompanied by the dissociation of other PMe$_3$ ligand to afford [Fe(κ^2-*P*,*SiH*-**L26**-H)(PMe$_3$)$_2$] (**91-II**). Finally, the electron-rich iron(0) center activates the Si–H bond *via* oxidative addition to form **91** upon coordination of one molecule of PMe$_3$ (Scheme 32). The iron(II) species **91** showed high catalytic activity for the reduction of aldehydes and ketones with hydrosilanes, as well as, for the reduction of benzamide to cyanobenzene with HSi(OEt)$_3$. Furthermore, catalyst **91** is able to selectively catalyse the reduction of α,β-unsaturated carbonyls to the corresponding α,β-unsaturated alcohols.[46]

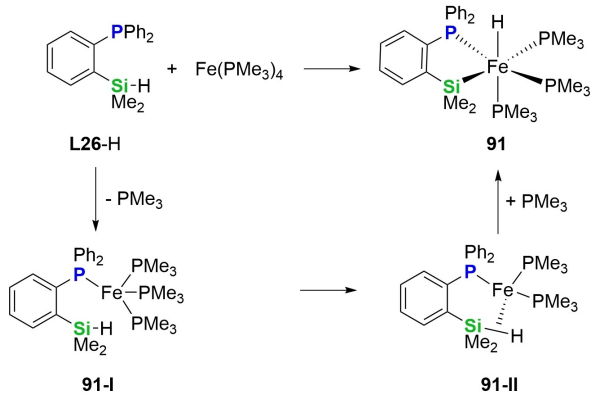

Scheme 32. Proposed mechanism for the formation of **91**.

More recently, Huertos and coworkers reported the synthesis of rhodium and iridium complexes with the (κ^2-*P*,*Si*-**L26**) ligand.[47] The reaction of dimers [{M(coe)$_2$}$_2$(μ-Cl)$_2$] (M = Rh, Ir) with 4 equivalents of the proligand **L26**-H led to the formation of the corresponding complex [M(Cl)(κ^2-*P*,*Si*-**L26**)$_2$] (M = Rh, **92**; Ir, **93**). When the Rh derivative **92** was treated with NaBAr$^F_4$ in CH_2Cl_2 followed by addition of a small amount of CH_3CN, the cationic rhodium derivative [Rh(κ^2-*P*,*Si*-**L26**)$_2$(NCCH$_3$)][BAr$^F_4$] (**94**) was formed. A related iridium cationic compound [Ir(κ^2-*P*,*Si*-**L26**)$_2$(NC CH$_3$)$_2$][BAr$^F_4$] (**95**) bearing two coordinated CH_3CN molecules was obtained when the reaction of **93** and NaBAr$^F_4$ was performed under the same reaction conditions (Scheme 33). The metal–Si bond distances in complexes **92**, **93**,

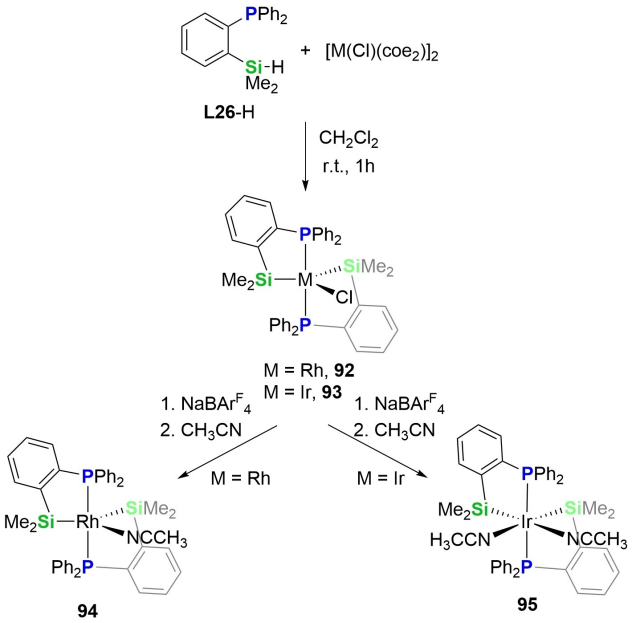

Scheme 33. Synthesis of complexes **92**, **93**, **94** and **95**.

94 and **95** are in the range expected for metal–silyl bonds (Table 2). These four complexes (**92**, **93**, **94** and **95**) are active

catalysts in the hydrolysis of dihydrosilanes to give the corresponding silanol, silanediol or hidrosiloxane products selectively, depending on the catalyst/substrate combination. The authors postulate that the electronic nature of both catalyst and substrate controls the selectivity of the hydrolytic processes, while steric factors influence condensation events.[47]

Smith and coworkers reported the proligand *o*-HSi(^{i}Pr)$_2$(P(*p*-Tolyl)$_2$)C$_6$H$_4$ (**L27**-H), related to **L26**-H but with isopropyl and *p*-tolyl substituents at the silicon and phosphorous atoms, respectively.[48] The proligand **L27**-H was designed to create an electron-rich framework that could facilitate C–H cleavage. The reaction of **L27**-H with [{Ir(cod)}$_2$(μ-OMe)$_2$] gives the complex [Ir(κ^2-*P*,*Si*-**L27**)(cod)] (**96**) (Scheme 34). The structure of the Ir(I)

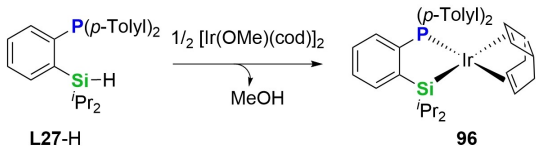

Scheme 34. Synthesis of the Ir-(κ^2-*P*,*Si*) complex **96**.

complex **96** is square-planar with the Ir–Si bond distance of 2.376(2) Å, typical for a Ir–silyl bond. Complex **96** has been found to be active as homogeneous catalyst for the borylation of a broad range of substituted aromatic compounds.[48]

The κ^2(*Si*,*P*)-SiMe$_2$PCy$_2$C$_6$H$_4$ (**L28**) ligand, related to **L26** but with cyclohexyl substituents at the phosphorus atom instead of phenyl groups, was generated *in situ* due to an unusual ligand rearrangement of [M(κ^3-*P*,*Si*,*P*)(Me)] (M = Ni, Pd) species that involves Si–C(sp^3) bond formation to generate a M(0) intermediate followed by a Si–C(sp^2) oxidative addition to the metal centre to afford the corresponding complex [M(κ^2-*P*,*Si*-**L28**)(κ^2-*P*,*C*-o-C$_6$H$_4$PCy$_2$)] (M = Pd, **97**; Ni, **98**). In the case of nickel complex **98**, these Si–C bond activation processes are reversible. Palladium complex **97** could be also obtained by direct reaction of (2-Cy$_2$PC$_6$H$_4$)$_2$SiMe$_2$ with 0.5 equivalents of [Pd$_2$(dba)$_3$] (Scheme 35).[49]

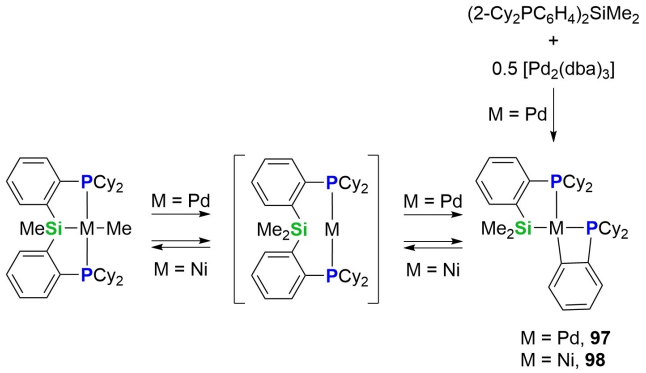

Scheme 35. Synthesis of complexes **97** and **98**.

Same group published the first *P*,*Si*,*N* mixed-donor silyl pincer ligand (**L29**) derived from the precursor SiHMe(2-^{t}Bu$_2$PC$_6$H$_4$)(2-Me$_2$NC$_6$H$_4$) (**L29**-H).[50] The authors found that the amino donor of this molecule is labile and the hemilability of the *P*,*Si*,*N* ligand promotes the isolation of the Pd- and Pt-(κ^2-*P*,*Si*) complexes [M(X)(κ^2-*P*,*Si*-**L29**)(PMe$_3$)] (M = Pd, X = Br; **99**; M = Pt, X = Cl; **100**). These group 10 complexes were synthetized by reaction of PdBr$_2$ or PtCl$_2$(cod) with **L29**-H in the presence of NEt$_3$ to give the corresponding square planar complexes [M(X)(κ^3-*P*,*Si*,*N*-**L29**)]. The addition of PMe$_3$ produces the selective displacement of the amine arm from the metal center to give **99** or **100**, respectively (Scheme 36). A related

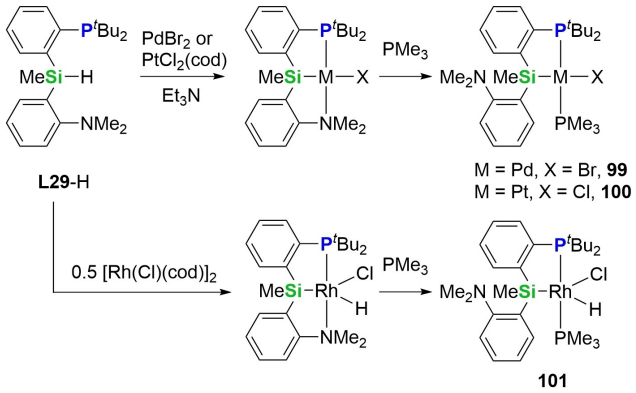

Scheme 36. Synthesis of complexes **99**, **100** and **101**.

rhodium complex was obtained following similar reaction sequence. Thus, [Rh(H)(Cl)(κ^3-*P*,*Si*,*N*-**L29**)] was obtained from reaction of the dimer [{Rh(cod)}$_2$(μ-Cl)$_2$] with **L29**-H. Then, addition of PMe$_3$ led to the quantitative formation of [Rh(H)(Cl)(κ^3-*P*,*Si*-**L29**)(PMe$_3$)] (**101**) (Scheme 36).[50]

Recently, He *et al.* have published an efficient one-pot method for the synthesis of P-atropisomeric Si-stereogenic monohydrosilanes with excellent stereoselectivity.[51] To prove the potential of the new chiral phosphine Si-stereogenic monohydrosilane as ligands, reactions with different metal fragments were tested. Treatment of [{M(cod)}$_2$(μ-Cl)$_2$] (M = Rh or Ir) with 4 equivalents of two different phosphine-based monohydrosilanes **L30**-H and **L31**-H in toluene at room temperature gave the chiral metal-silicon air-stable complexes **102** (Rh) and **103** (Ir) respectively (Scheme 37).

2.3. Transition Metal Complexes with κ^2-*S*,*Si* and κ^2-*O*,*Si* Ligands

The first examples of TM-(κ^2-*S*,*Si*) complexes were reported in 2015 by Huertos *et al.* They prepared the rhodium(III) dinuclear complex [Rh(κ^2-*S*,*Si*-**L32**)$_2$}$_2$(μ-Cl)$_2$] (**104**) by reaction of four equivalents of the proligand SiMe$_2$H(o-C$_6$H$_4$SMe) (**L32**-H) with [{Rh(cod)}$_2$(μ-Cl)$_2$] in CH$_2$Cl$_2$ (Scheme 38).[52] The formation of **104** takes place *via* the Rh(I)/Rh(III) mixed-valent species [{Rh(κ^2-*S*,*Si*-**L32**)}{Rh(cod)}(μ-Cl)$_2$] (**105**), which could be isolated from the reaction of [{Rh(cod)}$_2$(μ-Cl)$_2$] with two equivalents of **L32**-H.[52]

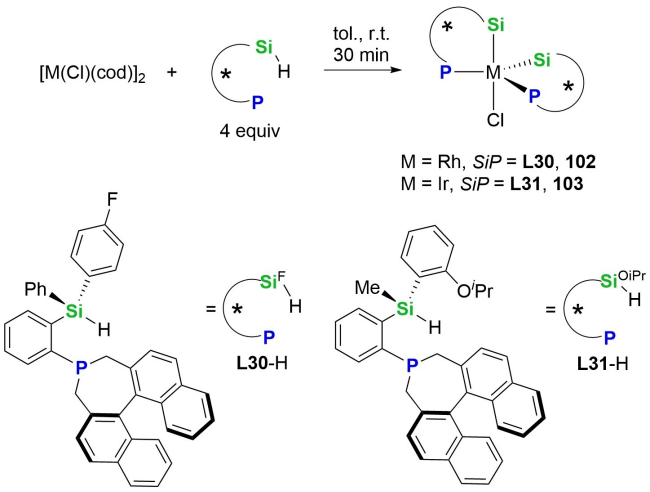

Scheme 37. Synthesis of complexes **102** and **103**.

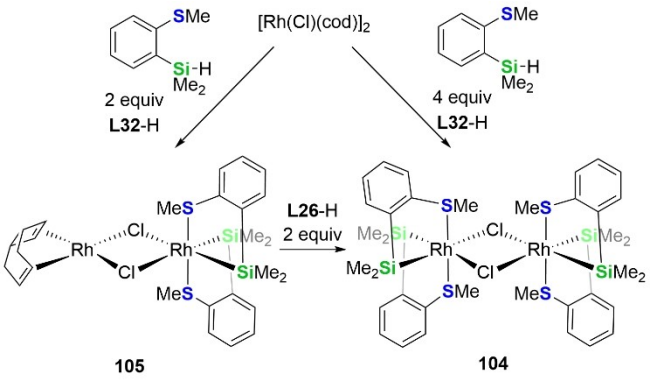

Scheme 38. Synthesis of the complexes **104** and **105**.

The Rh–Si bond distances in **104**, 2.3154(11) Å and 2.3104(10) Å, and in **105**, 2.2992(9) Å and 2.3030(9) (10) Å, clearly show the silyl character of these bonds (Table 3).[2b,c,d]

In subsequent studies, Huertos *et al.* prepared the cationic complex [Rh(H)(κ²-*S*,*Si*-**L32**)(PPh$_3$)$_2$][BAr^F$_4$] (**106**) by reaction of the proligand **L32**-H with [Rh(Cl)(PPh$_3$)$_3$] and NaBAr^F$_4$ in CH_2Cl_2 at r.t. (Scheme 39).[53] Complex **106** has shown to be an effective catalyst precursor for the solvent-free tandem isomerization-hydrosilylation of internal olefins, showing complete selectivity to the formation of silanes with linear alkyl chains.[53] Moreover, **106** also catalyzed the reduction of alkyl halides with triethylsilane. These reactions are performed in a solvent-free manner. Few years later, Huertos *et al.* prepared the family of proligands [SiMe$_2$H(o-C$_6$H$_4$SR)] (R = ^{i}Bu, **L33**-H; pentyl, **L34**-H; benzyl, **L35**-H; neopentyl, **L36**-H), related to **L32**-H but with different substituents on the sulfur atom.[54] The reaction of the proligand (**L33**-H, **L34**-H, **L35**-H or **L36**-H) with [Rh(Cl)(PPh$_3$)$_3$] and NaBAr^F$_4$ in CH_2Cl_2 affords the corresponding cationic species [Rh(H)(κ²-*S*,*Si*-**Ln**)(PPh$_3$)$_2$][BAr^F$_4$] (**Ln** = **L33**, **107**; **L34**, **108**; **L35**, **109**; **L36**, **110**) (Scheme 39).[54] These new cationic Rh(III) compounds, (**106**-**110**) have proved to be efficient catalysts for the solvent-free tandem isomerization-hydrosilylation reaction of alkenes forming the anti-Markovnikov terminal silyl alkanes as the only silylated products.[54]

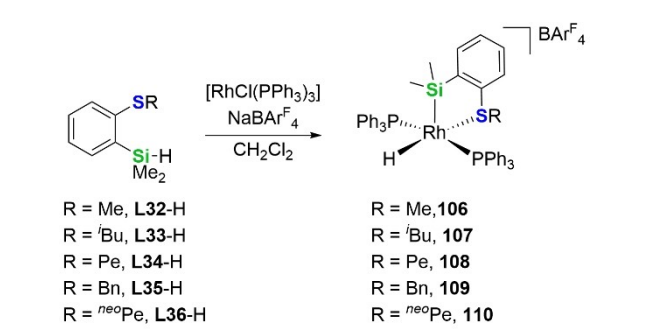

Scheme 39. Synthesis of the Rh-(κ²-*S*,*Si*) complexes **106–110**.

Ghosh *et al.* have recently reported the *in situ* preparation of the ligands {κ²-*S*,*Si*-(NSiPhR)(S$_2$C$_7$H$_4$)} (R = H, **L37**; Ph, **L38**) by the thermal reaction of the ruthenium borate species [Ru(κ²-*N*,*S*-C$_7$H$_4$NS$_2$){κ³-H,S,S′-H$_2$B(C$_7$H$_4$NS$_2$)$_2$}PPh$_3$] with PhRSiH$_2$ (R = H, Ph). The reaction with one equivalent of PhRSiH$_2$ in toluene at 333 K led to a mixture of complexes including [Ru{κ²-*S*,*Si*-(**Ln**)}{κ³-*H*,*S*,*S*′-H$_2$B(C$_7$H$_4$NS$_2$)$_2$}(PPh$_3$)] (**Ln** = **L37**, **111 a/b**; **L38, 112 a/b**) and the hydridotrisilyl complex [Ru(H)(κ²-*S*,*Si*-(**L38**)$_3$] (**113**) (Scheme 40). However, the reaction with excess (3 equiv) of

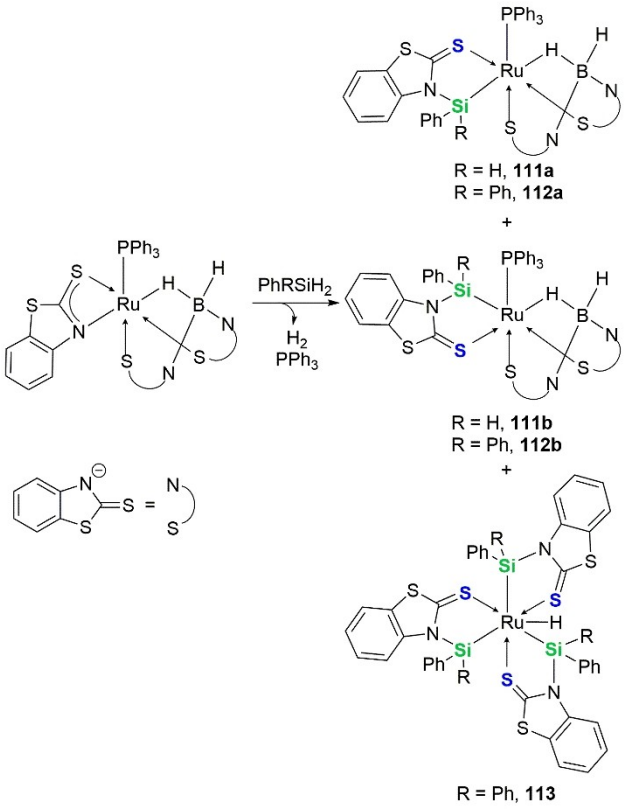

Scheme 40. Reactivity of [Ru(κ²-*N*,*S*-C$_7$H$_4$NS$_2$){κ³-*H*,*S*,*S*′-H$_2$B(C$_7$H$_4$NS$_2$)$_2$}PPh$_3$] with PhRSiH$_2$ (R = H, Ph).

Ph_2SiH_2 at 363 K selectively affords [Ru(H){κ²-*S*,*Si*-(**L38**}$_3$] (**113**), which was also selectively obtained by addition of excess of Ph_2SiH_2 to a mixture of complexes **112a**/**b**.[55]

Examples of TM-complexes with κ²-(*O*,*Si*) ligands are also known. Roper, Wright and collaborators reported the reaction of [Ru(SiClPh$_2$)(κ²-S$_2$CNMe$_2$)(CO)(PPh$_3$)$_2$] with thallium acetate to afford the ruthenium complex [Ru(κ²-*O*,*Si*-Si(OC(O)Me)Ph$_2$)(κ²-S$_2$CNMe$_2$)(CO)(PPh$_3$)] (**114**) by nucleophilic substitution at the Si–Cl by acetate favored by the precipitation of TlCl (Scheme 41).[18]

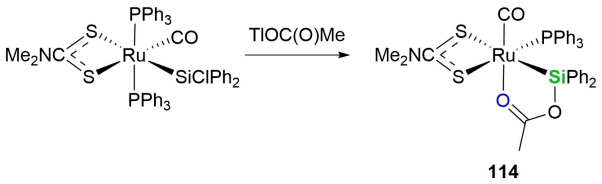

Scheme 41. Synthesis of the Ru-(κ²-*O*,*Si*) complex **114**.

Recently, Hass *et al.* reported a stable Ti(III) species, [TiCp$_2${κ²-*O*,*Si*-(Si{Si(OMe)$_3$}$_2$-Si(OMe)$_2$-OMe)] (**115**), when attempted disilylation of titanocenedichloride with 2 equivalents of potassium tris(trimethoxysilyl)silanide [(MeO)$_3$Si]$_3$SiK (Scheme 42).[56] This radical is stabilized by donation of a lone

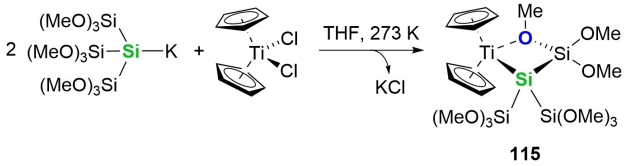

Scheme 42. Synthesis of the Ti-(κ²-*O*,*Si*) complex **115**.

pair of one oxygen atom of a methoxy group giving rise to κ²-(*O*,*Si*) coordination mode. The Ti–Si bond length (2.7432(7) Å) is significantly increased compared to related chloro-Ti(IV) complex [TiCp$_2$Cl{Si(Si(MeO)$_3$)$_3$}] (2.7037(7) Å) (Table 4).

2.4. Transition Metal Complexes with κ²-*C*,*Si* Ligands

Silyl and *N*-heterocyclic carbene (NHCs) ligands are strongly σ-donating ligands with a strong *trans*-effect. Examples of TM-complexes with functionalized NHC ligands featuring silyl donors groups have remained difficult to catch, although some NHCs with silyl substituents on the imidazole ring are known. Deng *et al.* reported in 2013 that the reaction of the cyclometallated iron(II) complex [Fe(IMes′)$_2$Fe] (IMes′ = cyclometalated IMes ligand, IMes = 1,3-dimesitylimidazol-2-ylidene) with $PhMeSiH_2$ or Ph_2SiH_2 at r.t. leads to the corresponidng silylated product [Fe(κ²-*C*,*Si*-SiPhR-IMes′)(IMes′)] (R = Me, **116**; Ph, **117**) (Scheme 43).[57]

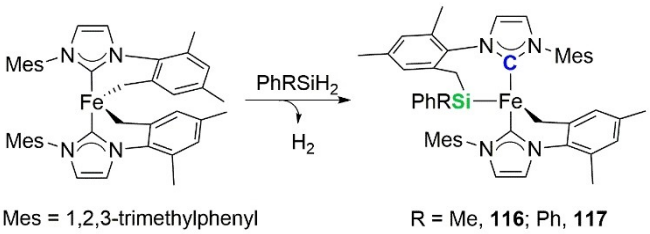

Scheme 43. Synthesis of the complexes [Fe(κ²-*C*,*Si*-SiPhR-IMes′)(IMes′)] (R = Me, **116**; Ph, **117**).

Deng *et al.* showed that this methodology can also be applied to cobalt. They found that [Co(IMes′)$_2$] reacts slowly with $PhSiH_3$ in benzene at r.t. to give the complex [Co(κ²-*C*,*Si*-SiPhH-IMes′)(IMes′)] (**118**). Analogously, the reactions of [Co(IMes′)$_2$] with $PhMeSiH_2$ and Ph_2SiH_2 in benzene proceeded very slowly at r.t. to afford the corresponding complex [Co(κ²-*C*,*Si*-SiPhH-IMes′)(IMes′)] (R = Me, **119**; Ph, **120**). It should be mentioned that when the reaction mixtures were heated to 343 K the formation of complexes **119** and **120** was achieved in 4 hours (Scheme 44).[58]

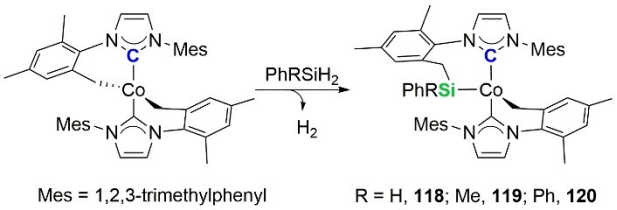

Scheme 44. Synthesis of the complexes [Co(κ²-*C*,*Si*-SiPhH-IMes′)(IMes′)] (R = H, **118**; Me, **119**; Ph, **120**).

Through some experiments on the reactivity of **118**, they found that in the presence of H_2 complex **118** is in equilibrium with the Co–H species [Co(H)(κ²-*C*,*Si*-SiPhH-IMes′)(IMes)] (**121**). The reaction of **118** with BH_3-thf leads to the species [Co(H)(κ²-*C*,*Si*-SiPhH-IMes′)(κ³-*C*,H_2*B*-BH_3-IMes′)] (**122**) (Scheme 45).[58] Preliminary studies showed that complex **118** catalyzed the hydrosilylation of 1-octene with $PhSiH_3$ with high activity and selectivity.[58] Deng *et al.* reported the synthesis of Co complexes with polydentate NHC-silyl ligands by reaction of **122** with 2-pyridone.[59] Moreover, the reaction of **122** with [FeCp$_2$][BPh$_4$] affords Co complexes with tridentate NHC–Si-NHC ligands.[60]

Conejero *et al.* reported that the cationic platinum cyclometallated *N*-heterocyclic carbene complex [Pt(I^{t}Bu^{i}Pr′)(I^{t}Bu^{i}Pr)][BAr$^F_4$] (I^{t}Bu^{i}Pr′ = cyclometalated I^{t}Bu^{i}Pr ligand, I^{t}Bu^{i}Pr = 1-*tert*-butyl-3-isopropylimidazol-2-ylidene) reacts with primary silanes $RSiH_3$ (R = Ph, ^{n}Bu) leading to the cyclometallated platinum(II) silyl-NHC complexes [Pt{κ²-*C*,*Si*-(SiHRCH$_2$CMe$_2$-NHC-^{i}Pr)}(I^{t}Bu^{i}Pr)][BAr$^F_4$] (R = Ph, **123**; R = ^{n}Bu, **124**) (Scheme 46).[61]

Similarly, the platinum(II) complexes [Pt(IMes′)(IMes)][BAr^F], and [Pt(IMes*′)(IMes*)][BAr^F], (IMes* = 1,3- dimesityl-4,5-dimethylimidazol-2-ylidene) react very fast with primary silanes $RSiH_3$ at

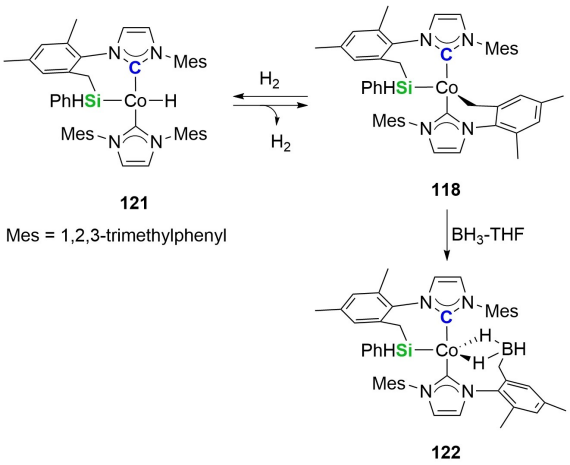

Scheme 45. Reactivity of **118** with H_2 and BH_3-thf.

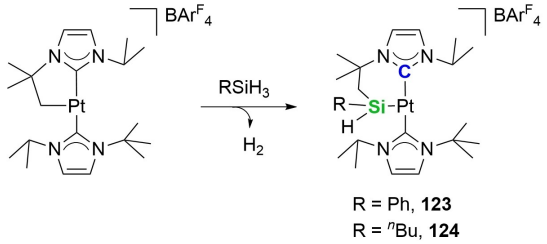

Scheme 46. Synthesis of the Pt(II) NHC-silyl complexes **123** and **124**.

r.t. to generate the corresponding silyl-cyclometallated complexes **125**, **126**, **127** and **128** (Scheme 47).[61]

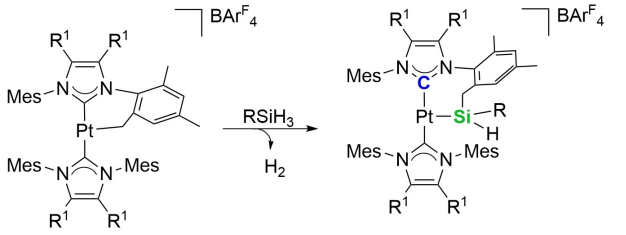

Scheme 47. Synthesis of the Pt(II) NHC-silyl complexes **125**, **126**, **127** and **128**.

2.5. Transition Metal Complexes with κ²-E,Si (E = Si, Ge, Sn) Ligands

Unsaturated tetryl species (silyl, germyl or stannyl) are inherently stronger σ-donors than the corresponding carbon species, while enhancing π-accepting character on going down in the group. In 2020, Scheschkewitz's group reported first TM-(κ²-*E*,*Si*) complexes.[62] Reaction of siliconoids functionalized with a tetrylene side-arm (E = Si, **L37**; Ge, **L38**; Sn, **L39**) towards $[\{Ir(coe)_2\}_2(\mu\text{-}Cl)_2]$ afforded the corresponding κ²-*E*,*Si* tetrylene-Si_6 iridium complexes (E = Si, **129**; Ge, **130**; Sn, **131**) (Scheme 48).

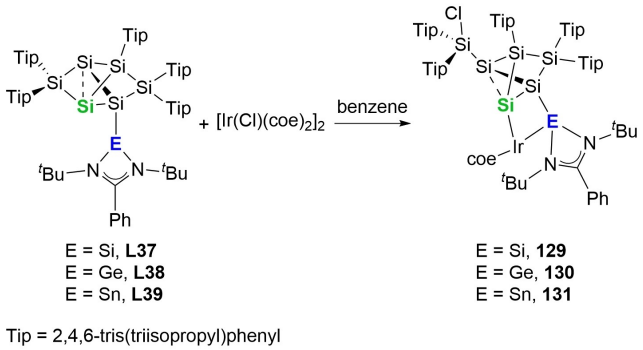

Scheme 48. Synthesis of complexes **129**, **130** and **131**.

Authors propose a mechanism for the formation of these complexes starting with coordination of the pendant tetrylene atom of the ligand to the metal and subsequnent oxidative addition of a Si–E single bond. Then, reductive elimination of the chlorine atom and $Si(Tip)_2$ (Tip = 2,4,6-tris(isopropyl)phenyl) fragment gives the final products with a exohedral chlorosilyl group. The Ir–Si(silyl) bond lengths 2.320(1) Å for **129** and 2.3517(7) Å for **130** and Ir–E 2.334(1) Å (E = Si, **129**) and 2.4113(3) Å (E = Ge, **130**) are those of single bonds (Table 6). All complexes have proven to be active catalysts for isomerization of terminal alkenes to 2-alkenes.

Recently, Maron, Jones and coworkers published the synthesis of first silicon analogue of an abnormal *N*-heterocyclic carbene.[63] Insertion of CO into the Si–N bond of the aminidate-stabilized 1,2-disilylene $[\{ArC(NDip)_2\}Si]_2$ (Dip = 2,6-diisopropylphenyl, Ar = 4-$C_6H_4{}^t$Bu), and Si–Si bond cleavage affords disilylene **L40**. $Mo(CO)_6$ reacts with **L40** under UV light at r.t. to give the chelated bis(silylene) molybdenum complex **132** (Scheme 49). This complex can also be obtained from reaction

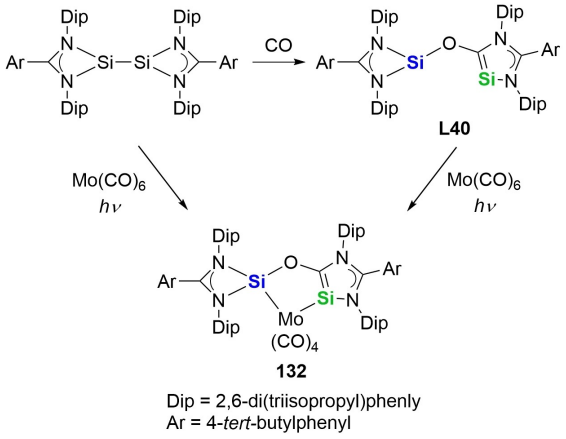

Scheme 49. Synthesis of the Mo-(κ²-*Si*,*Si*) complex **132**.

of [{ArC(NDip)$_2$}Si]$_2$ with Mo(CO)$_6$ under irradiation conditions suggesting that CO dissociated from Mo(CO)$_6$ reacts with the disilylene to give **L40**, which reacts with molybdenum carbonyl species affording **132**. Complex **132** was characterized by X-ray diffraction analysis and molecular structure shows silicon centers chelating a Mo(CO)$_4$ fragment in a *cis*-fashion to give a five-membered ring. The reported Mo–Si bond distances 2.478(2) and 2.5186(15) Å (Table 6) are in the known range for neutral silylene molybdenum carbonyl complexes (2.447–2.578 Å).[63]

3. Analysis of metal–Si distances in TM-(κ^2-*L*,*Si*) complexes

Tables 1 to 6 show the metal–Si bond distances reported for the complexes included in this review. All of them fall within the usual range of distances for metal–silyl bonds.[2b,c,d,65] Stablishing a general trend of behavior is difficult because not many examples of this type of complexes have been published to date. However, in the case of rhodium and iridium complexes with κ^2-*N*,*Si* and κ^2-*P*,*Si* ligands there are enough examples to illustrate that, regardless of the silicon substituents and the nature of linker, the metal–Si bond distances in Rh- and Ir-(κ^2-*N*,*Si*) species are shorter than in related Rh- and Ir-(κ^2-*P*,*Si*) complexes. This behavior could be due to a greater σ-donor character of the phosphine moiety in κ^2-*P*,*Si* ligands compared to the nitrogen of the corresponding κ^2-*N*,*Si* ligand.

TM-complexes with monoanionic κ^2-pyridine-2-yloxy-silyl based exhibit short metal–Si bond distances, between 2.23-2.29 Å (for Rh) and 2.25-2.29 Å (for Ir) (Table 1). This was the reason for some authors to propose them as examples of base-stabilized metal–silylene bonds.[16,17,18] In this regards, our group published in 2020 a QTAIM analysis of the Ir–Si bond in 2-pyridone-stabilized silyl iridium complexes, which allowed to conclude that the Ir–Si bonds in these complexes can be considered as an intermediate between the base-stabilized silylene and silyl cases.[20] Theoretical calculations based on Energy Decomposition Analysis (EDA) in combination with the Natural Orbital for Chemical Valence (NOCV) were performed for Ir-(κ^3-*N*,*Si*,*N*),[64] Ir-(κ^2-*N*,*Si*)[26] and Rh-(κ^2-*N*,*Si*)[29] complexes. The obtained results showed the covalent nature of the metal–Si bond and the significant role of electrostatic interactions on it. Indeed, the electrostatic component of the bond has been found to be almost twice as strong as the total orbital interactions. This fact indicates a highly polarized covalent bond, which can explain the shortening of M–Si (M = Rh, Ir) bond distances in these type of complexes.

Therefore, in all the examples collected in this review the metal-silicon bond distance falls within the range of distances that would be expected for metal–silyl bonds.[2b,c,d,65] Although in some cases, metal–Si bond distances shorter than expected have been observed. The bond shortening is mainly due to the ionic component contribution since the backbonding from d orbitals of the metal to the σ* orbitals of the silicon is considerably low.[26,29,64]

Table 1. Selection of metal–Si bond distances reported for TM-(κ^2-*N*,*Si*)$_n$ (n = 1, 2, 3) complexes.

M–Si	Complex	Bond-distance (Å)	Number of κ^2-*L*,*Si* ligands	Ref.
Co–Si	13[a]	2.2375(9) (A) 2.2311(8) (A) 2.2392(9) (A) 2.2315(8) (B) 2.2424(9) (B) 2.2404(9) (B)	3	[11]
Rh–Si	**2**	2.2571(6) 2.2500(6)	2	[12]
Rh–Si	**5**	2.278(1) 2.290(1) 2.301(1)	3	[10b]
Rh–Si	**16**	2.2746(7) 2.2654(8)	2	[12]
Rh–Si	**17**	2.2573(8) 2.2498(8)	2	[12]
Rh–Si	**19**	2.2635(7)	1	[13]
Rh–Si	**22**	2.2985(7)	1	[13]
Rh–Si	**24**	2.2648(4)	1	[15a]
Rh–Si	**25**	2.2990(8)	1	[15a]
Rh–Si	**45**	2.2277(8) 2.2388(10)	2	[25]
Rh–Si	**56**	2.2907(6)	1	[29]
Rh–Si	**57**	2.2738(3)	1	[29]
Rh–Si	**58**	2.2689(3)	1	[29]

Table 1. continued

M–Si	Complex	Bond-distance (Å)	Number of κ^2-*L*,*Si* ligands	Ref.
Ir–Si	**6**	2.296(4) 2.301(4) 2.305(4)	3	[10b]
Ir–Si	**26**	2.3016(10)	1	[15b]
Ir–Si	**27**	2.2887(14)	1	[15b]
Ir–Si	**37**	2.2634(14) 2.2695(14) 2.2552(14) 2.2747(14)	2	[19]
Ir–Si	**38**[a]	2.2515(7) (A) 2.2579(7) (A) 2.2499(7) (B) 2.2700(7) (B)	2	[20]
Ir–Si	**39**	2.2853(6)	1	[21]
Ir–Si	**40**	2.2645(10) 2.2505(11)	2	[19]
Ir–Si	**41**	2.2702(10) 2.2668(11)	2	[20]
Ir–Si	**42**	2.2570(5) 2.2615(5)	2	[22]
Ir–Si	**43**	2.2573(8) 2.2498(8)	2	[20]
Ir–Si	**47**	2.2792(3)	1	[26]
Ir–Si	**48**	2.2814(4)	1	[26]
Ir–Si	**49**	2.2835(5)	1	[26]
Ir–Si	**51**	2.2915(6)	1	[26]
Ir–Si	**53**	2.2876(4)	1	[26]
Ir–Si	**55**	2.2731(12)	1	[27a]
Fe–Si	**32**	2.2640(10)	1	[16b]
Fe–Si	**60**	2.246(1)	1	[30]
Fe–Si	**62**	2.2455(7)	1	[30]
Fe–Si	**63**	2.2166(5)	1	[30]
Fe–Si	**64**	2.2248(6)	1	[30]
Fe–Si	**65**	2.2338(5)	1	[30]
Ru–Si	**35**	2.3487(4)	1	[18]
Ru–Si	**36**	2.3400(7)	1	[18]
Ru–Si	**66**	2.3809(7)	1	[31]
Ru–Si	**67**	2.3213(5) 2.3264(5)	3	[31]
Ru–Si	**68**	2.3283(5)	2	[31]
W–Si	**34**	2.5072(10)	1	[17]

[a] The unit cell contains two independent molecules (A and B).

Table 2. Selection of metal–Si bond distances reported for TM-(κ^2-*P*,*Si*)$_n$ (n = 1, 2) complexes.

M–Si	Complex	Bond-distance (Å)	Number of κ^2-*L*,*Si* ligands	Ref.
Co–Si	**87**	2.3353(5)	1	[43]
Co–Si	**88**	2.2735(10)	1	[43]
Co–Si	**89**	2.3368(9)	1	[43]
Rh–Si	**92**	2.3099(6)	2	[47]
Rh–Si	**94**	2.341(1) 2.311(1)	2	[47]
Rh–Si	**102**	2.300(1) 2.300(2)	2	[51]
Ir–Si	**74**	2.3337(8) 2.3451(9)	2	[36]
Ir–Si	**75**	2.3233(18)	2	[38]
Ir–Si	**93**	2.319(5) 2.325(5)	2	[47]
Ir–Si	**95**	2.356(1) 2.366(1)	2	[47]
Ir–Si	**96**	2.376(2)	1	[48]
Ir–Si	**103**	2.338(4) 2.310(4)	2	[51]
Ru–Si	**76 b**	2.4240(11) 2.4647(11)	2	[38]
Ru–Si	**85 b**	2.352(3)	1	[42]
Os–Si	**83**	2.4716(13)	1	[41]
Os–Si	**84**	2.5110(8)	1	[41]
Pd–Si	**72**	2.3331(7) 2.3326(6)	1	[36]
Pd–Si	**80 c**	2.361(2) 2.358(2)	2	[39]
Pd–Si	**97**	2.3037(4)	1	[50]
Pt–Si	**71 b**	2.368(6) 2.342(8)	2	[34]
Pt–Si	**77 a**	2.408(1)	2	[39]
Pt–Si	**78 a**	2.3492(2) 2.3532(2)	2	[39]
Pt–Si	**78 c**	2.361(2) 2.361(1)	2	[39]
Pt–Si	**81**	2.307(2)	1	[39]
Pt–Si	**82**	2.3228(2)	1	[39]
Pt–Si	**100**	2.3077(9)	1	[50]

Table 3. Selection of metal–Si bond distances reported for TM-(κ^2-*S*,*Si*)$_n$ (n = 1, 2, 3) complexes.

M–Si	Complex	Bond-distance (Å)	Number of κ^2-*L*,*Si* ligands	Ref.
Rh–Si	**104**	2.3154(11) 2.3104(10)	2	[52]
Rh–Si	**105**	2.2992(9) 2.3030(8)	2	[52]
Ru–Si	**111 a**	2.300(4)	1	[55]
Ru–Si	**113**	2.211(4) 2.364(4) 2.452(4)	3	[55]

Table 4. Selection of metal–Si bond distances reported for TM-(κ²-*O*,*Si*) complexes.

M–Si	Complex	Bond-distance (Å)	Number of κ²-*L*,*Si* ligands	ref
Ru–Si	**114**	2.3499(13)	1	[18]
Ti–Si	**115**	2.7432(7)	1	[56]

Table 5. Selection of metal–Si bond distances reported for TM-(κ²-*C*,*Si*) complexes.

M–Si	Complex	Bond-distance (Å)	Number of κ²-*L*,*Si* ligands	ref
Co–Si	**118**	2.300(2)	1	[58a]
Co–Si	**119**	2.309(1)	1	[58a]
Co–Si	**120**	2.327(1)	1	[58a]
Co–Si	**122**	2.274(1)	1	[58a]
Fe–Si	**116**	2.396(1)	1	[57]
Fe–Si	**117**	2.419(1)	1	[57]
Pt–Si	**123**	2.2693(1)	1	[61]
Pt–Si	**125**	2.2609(8)	1	[61]
Pt–Si	**126**	2.2619(6)	1	[61]

Table 6. Selection of metal–Si bond distances reported for TM-(κ²-*E*,*Si*) (E = Si, Ge) complexes.

M–Si	Complex	Bond-distance (Å)	E	ref
Ir–Si	**129**	2.320(1) 2.334(1)	Si	[62]
Ir–Si	**130**	2.3517(7)	Ge	[62]
Mo–Si	**132**	2.478(2) 2.5186(15)	Si	[63]

4. Summary and Outlook

This review shows that the chemistry of TM-complexes with monoanionic bidentate silyl (κ²-*L*,*Si*) ligands has experienced great development during the last decade. Among the properties of this type of ligands are their easy tunable σ-donor character, and the high *trans*-effect and -influence of the silyl group which facilitate the generation of electronically and coordinatively unsaturated species. There is still much room for improvement in this field, especially with respect to the chemistry of complexes with earth-abundant metals. In fact, most of the so far reported TM-(κ²-*L*,Si) species are complexes of Rh, Ir, Ru and Pt. Exceptionally, the chemistry of TM-complexes with κ²-*C*,*Si*-(silyl-NHC) ligands is dominated by Co, Fe and Pt complexes.

The most used synthetic methods for the preparation of TM-(κ²-*L*,*Si*) complexes include: (i) oxidative addition of the Si–H bond of the proligand assisted by the coordination of the L donor group; (ii) nucleophilic substitution of one of the silicon substituents in TM–silyl complexes and (iii) reaction of cyclometalated TM-(κ²-*C*,*C*-NHC) complexes with primary and / or secondary silanes. Among them, the assisted oxidative addition of the Si–H of the corresponding proligand stands out.

The metal–silyl bond distances in TM-(κ²-*L*,*Si*) complexes are in the expected range for metal–silyl bonding, therefore, they can be considered as X-type silyl ligands. Conversely, in the case of TM-(κ²-*N*,*Si*) complexes is frequent to find metal–Si bond distances shorter than it should be expected for a metal–silyl bond. Theoretical studies showed the electron-sharing nature of the covalent metal–Si bond, and that the shortening of the metal–Si bond can be explained on the basic of the significant role of electrostatic attractions between the TM fragment and the ligand.

The mechanisms of the catalytic processes promoted by TM-(κ²-*L*,*Si*) complexes are influenced by the nature of the ligand. Thus, while using TM-(κ²-*N*,*Si*) catalysts σ-bond metathesis mechanisms and σ-complex assisted metathesis (CAM) mechanisms are favored, TM-(κ²-*P*,*Si*)-catalyzed processes that follows oxidative addition/reductive elimination mechanisms are also possible. While the hemilabile character of κ²-(*N*,*Si*)-type ligands has not been published, examples of this character are known in TM-(κ²-*P*,*Si*) complexes.

Regarding the applications of this type of TM-compounds, it is worth mentioning that many of these complexes have proven to be effective catalysts in catalytic hydrosilylation processes of alkenes, amides, and CO_2, selective hydrogenation processes of olefins and silane hydrolysis processes. Interestingly, some TM-(κ²-*L*,*Si*) species have found to be most active than their TM-(κ³-*L*,*Si*,*L*) counterparts in CO_2 hydrosilylation processes (κ²-*N*,*Si vs* κ³-*N*,*Si*,*N*) and Kumada coupling processes (κ²-*P*,*Si vs* κ³-*P*,*Si*,*P*).

Although, the application of these systems in asymmetric catalytic processes has not been widely explored, recent publications in this regard suggest that the design of TM-(κ²-*L*,*Si*) chiral ligands to enhance enantioselectivities will be one of the lines of development of the chemistry of this type of complexes.

In conclusion, the chemistry of TM-(κ²-*L*,*Si*) is still in a growth stage and it is expected that in the coming years the number of successful catalytic processes based on TM-(κ²-*L*,*Si*) homogeneous catalysts will expand.

Acknowledgements

Financial support from projects PID2021-126212OB–I00 (AEI-Spain) and DGA/FSE project E42_23R (Gobierno de Aragón) is gratefully acknowledged. M. B. thanks to Campus Iberus and European Union's Horizon 2020 research and innovation program under the Marie Skłodowska program – Grant Agreement No. 101034288. A. G.-E. thankfully acknowledges Universidad de Zaragoza and Banco Santander for a predoctoral fellowship "Ayudas para iberoamericanos y ecuatoguineanos en Estudios de Doctorado. Universidad de Zaragoza – Santander Universidades (2022–2023)".

Conflict of Interests

The authors declare no conflict of interest.

Keywords: silyl complexes · monoanionic bidentate silyl ligands · polydentate silyl ligands · transition metal complexes

[1] R. J. Lundgren, M. Stradiotto, Key Concepts in Ligand Design. In Ligand Design in Metal Chemistry (Eds M. Stradiotto and R. J. Lundgren). Wiley, Weinheim, 2016.
[2] a) J. Gao, Y. Ge, C. He, *Chem. Soc. Rev.* **2024**, *53*, 4648–4673; b) J. Y. Corey, *Chem. Rev.* **2016**, *116*, 11291–11435; c) J. Y. Corey, *Chem. Rev.* **2011**, *111*, 863–1071; d) J. Y. Corey, J. Braddock-Wilking, *Chem. Rev.* **1999**, *99*, 175–292.
[3] M. T. Whited, B. L. H. Taylor, *Comments Inorg. Chem.* **2020**, *40*, 217–276.
[4] Selected reviews: a) J. A. Cabeza, P. García-Álvarez, *Chem. Eur. J.* **2023**, *29*, e202203096; b) T. Komuro, Y. Nakajima, J. Takaya, H. Hashimoto, *Coord. Chem. Rev.* **2022**, *473*, 214837; c) M. T. Whited, *Dalton Trans.* **2021**, *50*, 16443–16450; d) M. Simon, F. Breher, *Dalton Trans.* **2017**, *46*, 7976–7997; e) M. T. Whited, J. Zhang, S. Ma, B. D. Nguyen, D. E. Janzen, *Dalton Trans.* **2017**, *46*, 14757–14761; f) M. S. Balakrishna, P. Chandrasekaran, P. P. George, *Coord. Chem. Rev.* **2003**, *241*, 87–117.
[5] a) M. Tanabe, K. Osakada, *Transition Metal Complexes of Silicon (Excluding Silylene Complexes)*, Chapter 2, in *Organosilicon Compounds, Theory and Experiment (Synthesis)* (Ed.: V. Y. Lee), Academic Press, London, 2017; b) E. Sola, *Silicon-based pincers: trans influence and functionality*. Chapter 19, in *Pincer Compounds: Chemistry and Applications*, (Ed.: D. Morales-Morales) Elsevier, Amsterdam, 2018; c) L. Turculet, *PSiP transition-metal pincer complexes: synthesis, bond activation, and catalysis*, Chapter 6, in *Pincer and Pincer-Type Complexes: Applications in Organic Synthesis and Catalysis*, First Edition, (Eds.: K. J. Szabó, O. F. Wendt), Willey, Weinheim, 2014.
[6] For a review on TM-κ^2-*P,Si* complexes see: M. Okazaki, S. Ohshitanai, M. Iwata, H. Tobita, H. Ogino, *Coord. Chem. Rev.* **2002**, *226*, 167–178.
[7] a) J. Wagler, R. Gericke, *Polyhedron* **2023**, *245*, 116663; b) L. Ehrlich, R. Gericke, E. Brendler, J. Wagler, *Inorganics* **2018**, *6*, 119; doi: 10.3390/inorganics6040119.
[8] F. J. Fernández-Alvarez, R. Lalrempuia, L. A. Oro, *Coord. Chem. Rev.* **2017**, *350*, 49–60.
[9] H. G. Ang, W. L. Kwik, *J. Organomet. Chem.* **1989**, *361*, 27–30.
[10] a) P. I. Djurovich, A. Safir, N. Keder, R. J. Watts, *Coord. Chem. Rev.* **1991**, *111*, 201–214; b) P. I. Djurovich, A. L. Safir, N. L. Keder, R. J. Watts, *Inorg. Chem.* **1992**, *31*, 3195–3196; c) P. I. Djurovich, R. J. Watts, *Inorg. Chem.* **1993**, *32*, 4681–4682; d) P. I. Djurovich, R. J. Watts, *J. Phys. Chem.* **1994**, *98*, 396–397; e) P. I. Djurovich, W. Cook, R. Joshi, R. J. Watts, *J. Phys. Chem.* **1994**, *98*, 398–400.
[11] R. Imayoshi, H. Tanaka, Y. Matsuo, M. Yuki, K. Nakajima, K. Yoshizawa, Y. Nishibayashi, *Chem. Eur. J.* **2015**, *21*, 8905–8909.
[12] U. Prieto-Pascual, I. V. Alli, I. Bustos, I. J. Vitorica-Yrezabal, J. M. Matxain, Z. Freixa, M. A. Huertos, *Organometallics* **2023**, *42*, 2991–2998.
[13] U. Prieto-Pascual, A. Martínez de Morentin, D. Choquesillo-Lazarte, A. Rodríguez-Diéguez, Z. Freixa, M. A. Huertos, *Dalton Trans.* **2023**, *52*, 9090–9096.
[14] T. Komuro, D. Mochizuko, H. Hashimoto, H. Tobita, *Dalton Trans.* **2022**, *51*, 9983–9987.
[15] a) K. Sato, T. Komuro, H. Hashimoto, H. Tobita, *Chem. Lett.* **2020**, *49*, 1431–1434; b) K. Sato, T. Komuro, T. Osawa, H. Hashimoto, H. Tobita, *Organometallics* **2022**, *41*, 2612–2621.
[16] a) T. Sato, H. Tobita, H. Ogino, *Chem. Lett.* **2001**, 854–855; b) T. Sato, M. Okazaki, H. Tobita, H. Ogino, *J. Organomet. Chem.* **2003**, *669*, 189–199; c) T. Sato, M. Okazaki, H. Tobita, *Chem. Lett.* **2004**, 868–869.
[17] Y. Kanno, T. Komuro, H. Tobita, *Organometallics* **2015**, *34*, 3699–3705.
[18] W.-H. Kwok, G.-L. Lu, C. E. F. Rickard, W. R. Roper, L. J. Wright, *J. Organomet. Chem.* **2004**, *689*, 2979–2987.
[19] J. Guzmán, P. García-Orduña, V. Polo, F. J. Lahoz, L. A. Oro, F. J. Fernández-Alvarez, *Catal. Sci. Technol.* **2019**, *9*, 2858–2867.
[20] J. Guzmán, A. M. Bernal, P. García-Orduña, F. J. Lahoz, V. Polo, F. J. Fernández-Alvarez, *Dalton Trans.* **2020**, *49*, 17665–17673.
[21] J. Guzmán, A. M. Bernal, P. García-Orduña, F. J. Lahoz, L. A. Oro, F. J. Fernández-Alvarez, *Dalton Trans.* **2019**, *48*, 4255–4262.
[22] J. Guzmán, P. García-Orduña, F. J. Lahoz, F. J. Fernández-Alvarez, *RSC Adv.* **2020**, *10*, 9582–9586.
[23] J. Guzmán, A. Urriolabeitia, M. Padilla, P. García-Orduña, V. Polo, F. J. Fernández-Alvarez, *Inorg. Chem.* **2022**, *61*, 20216–20221.
[24] a) R. Lalrempuia, M. Iglesias, V. Polo, P. J. Sanz Miguel, F. J. Fernández-Alvarez, J. J. Pérez-Torrente, L. A. Oro, *Angew. Chem. Int. Ed.* **2012**, *51*, 12824–12827; b) A. Julián, E. A. Jaseer, K. Garcés, F. J. Fernández-Alvarez, P. García-Orduña, F. J. Lahoz, L. A. Oro, *Catal. Sci. Technol.* **2016**, *6*, 4410–4417; c) A. Julián, J. Guzmán, E. A. Jaseer, F. J. Fernández-Alvarez, R. Royo, V. Polo, P. García-Orduña, F. J. Lahoz, L. A. Oro, *Chem. Eur. J.* **2017**, *23*, 11898–11907.
[25] J. Guzmán, A. Torguet, P. García-Orduña, F. J. Lahoz, L. A. Oro, F. J. Fernández-Alvarez, *J. Organomet. Chem.* **2019**, *897*, 50–56.
[26] A. Gómez-España, P. García-Orduña, J. Guzmán, I. Fernández, F. J. Fernández-Alvarez, *Inorg. Chem.* **2022**, *61*, 16282–16294.
[27] a) A. Gomez-España, J. L. Lopez-Morales, B. Español-Sanchez, P. García-Orduña, F. J. Lahoz, M. Iglesias, F. J. Fernández-Alvarez, *Dalton Trans.* **2023**, *52*, 6722–6729; b) A. Gomez-España, J. L. Lopez-Morales, B. Español-Sanchez, P. García-Orduña, F. J. Lahoz, M. Iglesias, F. J. Fernández-Alvarez, *Dalton Trans.* **2023**, *52*, 11361–11362.
[28] J. Guzmán, A. Urriolabeitia, V. Polo, M. Fernández-Buenestado, M. Iglesias, F. J. Fernández-Alvarez, *Dalton Trans.* **2022**, *51*, 4386–4393.
[29] A. Gómez-España, P. García-Orduña, F. J. Lahoz, I. Fernández, F. J. Fernández-Álvarez, *Organometallics* **2024**, *43*, 402–413.
[30] Y. Shi, X. Li, T. Zheng, B. Xue, S. Zhang, H. Sun, O. Fuhr, D. Fenske, *Inorg. Chim. Acta* **2017**, *455*, 112–117.
[31] K. A. Smart, M. Grellier, L. Vendier, S. A. Mason, S. C. Capelli, A. Albinati, S. Sabo-Etienne, *Inorg. Chem.* **2013**, *52*, 2654–2661.
[32] T. D. Tilley. In The Chemistry of Orgainic Silicon. Compounds, S. Patai and Z. Rappoport (Eds.); Chap 24, p. 1415, Wiley, New York, 1989.
[33] J. Grobe, A. Walter, *J. Organomet. Chem.* **1977**, *140*, 325–348.
[34] R. D. Holmes-Smith, S. R. Stobart, T. S. Cameron, K. Jochem, *J. Chem. Soc. Chem. Commun.* **1981**, 937–939.
[35] R. Usui, Y. Sunada, *Inorg. Chem.* **2021**, *60*, 15101–15105.
[36] J. Shen, R. Usui, Y. Sunada, *Eur. J. Org. Chem.* **2022**, e202101563.
[37] A. García-Camprubí, M. Martín, E. Sola, *Inorg. Chem.* **2010**, *49*, 10649–10657.
[38] V. Montiel-Palma, O. Piechaczyk, A. Picot, A. Auffrant, L. Vendier, P. Le Floch, S. Sabo-Etienne, *Inorg. Chem.* **2008**, *47*, 8601–8603.
[39] Y.-J. Lee, J.-D. Lee, S.-J. Kim, S. Keum, J. Ko, I.-H. Suh, M. Cheong, S. O. Kang, *Organometallics* **2004**, *23*, 203–214.
[40] G. R. Clark, C. E. F. Rickard, W. R. Roper, D. M. Salter, L. J. Wright, *Pure Appl. Chem.* **1990**, *62*, 1039–1042.
[41] G. R. Clark, G.-L. Lu, C. E. F. Rickard, W. R. Roper, L. J. Wright, *J. Organomet. Chem.* **2005**, *690*, 3309–3320.
[42] H. Wada, H. Tobita, H. Ogino, *Organometallics* **1997**, *16*, 3870–3872.
[43] S. Xu, P. Zhang, X. Li, B. Xue, H. Sun, O. Fuhr, D. Fenske, *Chem. Asian J.* **2017**, *12*, 1234–1239.
[44] Z. Xiong, X. Li, S. Zhang, Y. Shi, H. Sun, *Organometallics* **2016**, *35*, 357–363.
[45] P. Zhang, S. Xu, X. Li, X. Qi, H. Sun, O. Fuhr, D. Fenske, *Polyhedron* **2018**, *143*, 165–170.
[46] S. Ren, S. Xie, T. Zheng, Y. Wang, S. Xu, B. Xue, X. Li, H. Sun, O. Fuhr, D. Fenske, *Dalton Trans.* **2018**, *47*, 4352–4359.
[47] U. Prieto-Pascual, A. Rodríguez-Diéguez, Z. Freixa, M. A. Huertos, *Inorg. Chem.* **2023**, *62*, 3095–3105.
[48] B. Ghaffari, S. M. Preshlock, D. L. Plattner, R. J. Staples, P. E. Maligres, S. W. Krska, R. E. Maleczka, M. R. III Smith, *J. Am. Chem. Soc.* **2014**, *136*, 14345–14348.
[49] S. J. Mitton, R. McDonald, L. Turculet, *Angew. Chem. Int. Ed.* **2009**, *48*, 8568–8571.
[50] A. J. Ruddy, S. J. Mitton, R. McDonald, L. Turculet, *Chem. Commun.* **2012**, *48*, 1159–1161.
[51] B. Yang, X. Tan, Y. Ge, Y. Li, C. He, *Org. Chem. Front.* **2023**, *10*, 4862–4870.
[52] S. Azpeitia, B. Fernández, M. A. Garralda, M. A. Huertos, *Eur. J. Inorg. Chem.* **2015**, 5451–5456.
[53] S. Azpeitia, M. A. Garralda, M. A. Huertos, *ChemCatChem* **2017**, *9*, 1901–1905.
[54] U. Prieto, S. Azpeitia, E. San Sebastian, Z. Freixa, M. A. Garralda, M. A. Huertos, *ChemCatChem* **2021**, *13*, 1403–1409.
[55] M. Zafar, R. Ramalakshmi, A. Ahmad, P. K. S. Antharjanam, S. Bontemps, S. Sabo-Etienne, S. Ghosh, *Inorg. Chem.* **2021**, *60*, 1183–1194.
[56] A. Sauermoser, T. Lainer, G. Glotz, F. Czerny, B. Schweda, R. C. Fischer, M. Haas, *Inorg. Chem.* **2022**, *61*, 14742–14751.
[57] Z. Ouyang, L. Deng, *Organometallics* **2013**, *32*, 7268–7271.

[58] a) Z. Mo, Y. Liu, L. Deng, *Angew. Chem. Int. Ed.* **2013**, *52*, 10845–10849; b) Z. Mo, L. Deng, *Synlett* **2014**, *25*, 1045–1049.
[59] J. Sun, C. Ou, C. Wang, M. Uchiyama, L. Deng, *Organometallics* **2015**, *34*, 1546–1551.
[60] J. Sun, L. Luo, Y. Luo, L. Deng, *Angew. Chem. Int. Ed.* **2017**, *56*, 2720–2724.
[61] P. Ríos, H. Fouilloux, J. Díez, P. Vidossich, A. Lledós, S. Conejero, *Chem. Eur. J.* **2019**, *25*, 11346–11345.
[62] N. E. Poitiers, L. Giarrana, V. Huch, M. Zimmer, D. Scheschkewitz, *Chem. Sci.* **2020**, *11*, 7782–7788.
[63] P. Garg, A. Carpentier, I. Douair, D. Dange, Y. Jiang, K. Yuvaraj, L. Maron, C. Jones, *Angew. Chem. Int. Ed.* **2022**, *61*, e202201705.
[64] P. García-Orduña, I. Fernández, L. A. Oro, F. J. Fernández-Álvarez, *Dalton Trans.* **2021**, *50*, 5951–5959.
[65] a) E. Lukevics, P. Arsenyan, O. Pudova, *Main Group Met. Chem.* **2002**, *25*, 415–436; b) E. Lukevics, P. Arsenyan, O. Pudova, *Main Group Met. Chem.* **2002**, *25*, 541–560; c) E. Lukevics, O. Pudova, *Main Group Met. Chem.* **2000**, *23*, 207–231; d) E. Lukevics, O. Pudova, *Main Group Met. Chem.* **1999**, *22*, 385–403.

Manuscript received: February 29, 2024
Revised manuscript received: May 22, 2024
Accepted manuscript online: May 23, 2024
Version of record online: ■■, ■■

REVIEW

This work summarizes the advances in the chemistry of transition metal complexes with monoanionic bidentate ligands κ^2-*L*,*Si* (*L* = *N*-heterocycle, phosphine, *N*-heterocyclic carbene, thioether, ester, silylether or tetrylene).

Dr. M. Batuecas, Dr. A. Goméz-España, Prof. Dr. F. J. Fernández-Álvarez**